Energy 294 (2024) 130803

Contents lists available at ScienceDirect

Energy

journal homepage: www.elsevier.com/locate/energy

4E analysis and triple objective NSGA-II optimization of a novel solar-driven combined ejector-enhanced power and two-stage cooling (EORC-TCRC) system

Hamed Mortazavi [a,b,**], Hamidreza Mortazavy Beni [c,*], Afshin Ahmadi Nadooshan [a], Mohammad S. Islam [d], Mohammad Ghalambaz [e]

[a] Department of Mechanical Engineering, Shahrekord University, Shahrekord, Iran
[b] Sefid Dasht Steel Complex, Shahrekord, Chaharmahal and Bakhtiari Province, Iran
[c] Department of Biomedical Engineering, Arsanjan Branch, Islamic Azad University, Arsanjan, Iran
[d] School of Mechanical and Mechatronic Engineering, University of Technology Sydney (UTS), 15 Broadway, Ultimo, NSW, 2007, Australia
[e] Laboratory on Convective Heat and Mass Transfer, Tomsk State University, Tomsk, Russia

ARTICLE INFO

Handling Editor: G Iglesias

Keywords:
4E analysis
Solar energy
Cogeneration cycle
NSGA-II
Multi-objective optimization
Cascade condenser

ABSTRACT

This study proposed an innovative combined ejector-enhanced organic Rankine cycle and two-stage compression refrigeration cycle (EORC-TCRC), to investigate its potential to revolutionize energy utilization and offer a sustainable solution for the current energy challenge. Energy, exergy, economic, and environmental (4E) analysis of the novel EORC-TCRC system was conducted first. The performance appraisal of the novel system compared to the conventional combined power and ejector refrigeration system has been evaluated. The evolutionary non-dominated Sort Genetic (NSGA-II) optimization algorithm was implemented to ascertain triple-objective optimal system operating conditions. The results revealed a significant improvement in refrigeration output, energy, and exergy efficiency with values of 220.06 kW, 11.67%, and 17.07%, respectively, compared to the conventional Rankine power and ejector refrigeration system. By different selections of the objective functions, four groups comprised of Multi-Objective C_T–η_{ex}, Multi-Objective C_T–η_{Th}, Multi-Objective η_{ex}–η_{Th}, and Triple-Objective mode presented to sought NSGA-II optimization results. The optimization results of Multi-Objective C_T–η_{Th} mode indicated that the best thermal efficiency and overall system cost rate operating conditions are 28.25% and 78,820 ($/year), respectively. While the optimal system operating condition occurs in the Triple-Objective η_{ex}- η_{Th}-C_T with the exergetic efficiency of 41.69%.

1. Introduction

In recent years, refrigeration has played an appreciable role in energy consumption in both domestic and industrial applications. The Compression Refrigeration Cycle (CRC) is one of the most accepted commercial refrigeration cycles that is widely used in many applications such as food and perishables storage, hospitals, HVAC, oil, gas, and petrochemical industries, liquefied gas production and cryogenic technology for producing pure oxygen and nitrogen for steel factories. Hence, it is essential to optimize refrigeration energy systems. Cogeneration power and refrigeration cycles are some of the best approaches to yield superior system optimal operation. In a conventional compression refrigeration system, there are two different parts in terms of pressure. One section is in the low pressure (between the expansion valve, evaporator, and compressor inlet), and one section is in the high pressure (after the compressor to the expansion valve). However, there are also one or more mid-pressure segments in a two- or multi-stage compression refrigeration cycle.

Nomenclature

Symbols		*Greeks*	
P	pressure (kPa)	η	efficiency
T	temperature (°C)	μ	entrainment ratio

(*continued on next page*)

* Corresponding author.
** Corresponding author. Sefid Dasht Steel Complex, Shahrekord, Chaharmahal and Bakhtiari Province, Iran.
E-mail addresses: h.mortazavi@sdsteel.ir, mortazavi.hamed.s@gmail.com (H. Mortazavi), HRM.Beni@iau.ac.ir, hrm.beni@gmail.com (H.M. Beni).

https://doi.org/10.1016/j.energy.2024.130803
Received 4 December 2023; Received in revised form 6 February 2024; Accepted 23 February 2024
Available online 25 February 2024

(*continued*)

Nomenclature

s	specific entropy (kJ/kg.K)	ϕ	maintenance cost factor
$\dot{W}$	power (kW)	φ	CO_2 mitigated per annum
$\dot{m}$	mass flow rate (kg/s)	ψ	CO_2 production
$\dot{Q}$	heat transfer rate (kW)		
h	specific enthalpy (kJ/kg)	*Superscript*	
$\dot{E}x$	exergy flow rate (kW)	n	system life time
$\dot{I}$	exergy destruction (kW)	el	electricity
u	velocity (m/s)		
U	overall heat transfer coefficient (kW/m^2K)	*Subscripts*	
F_C	correction factor	0	reference state
A	surface area (m^2)	Is	isentropic process
C	Overall cost function ($/year)	N	primary nozzle
Z	capital cost function ($)	M	mixing chamber
i	annual interest rate	D	diffuser section
		P	pump
Abbreviations		C	compressor
TCRC	Two-stage compression refrigeration cycle	T	turbine
EORC	Ejector-enhanced organic Rankine cycle	B	boiler
LMTD	logarithmic mean temperature difference	Ej	ejector
cas. cond	cascade condenser	S	isentropic
CRF	capital recovery factor	Se	separator
COP	coefficient of performance	cond	condenser
RCSs	Rankine cycle systems	evap	evaporator
NSGA	non-dominated Sort Genetic Algorithm	I	inlet
EES	Engineering Equation Solver	o	outlet
ORC	Organic Rankine Cycle	1; 2; 3; …. .	state points

Selbas et al. [1] investigated an exergy optimization to a superheated and subcooled vapor compression refrigeration cycle. They formulated thermodynamic properties using the artificial neural network methodology for three refrigerants, R-407c, R-134a, and R-22 and evaluated an optimal heat exchange surface corresponding to superheated and subcooled temperatures. Finally, a cost function is defined according to the optimal operating conditions. Sayyaadi and Nejatolahi [2] applied a multi-objective optimization on a vapor compression refrigeration cycle equipped with a cooling tower. By considering two objective functions, they optimized the vapor compression refrigeration cycle by three methods: thermodynamic, economical, and thermo-economical. They found that multi-objective thermoeconomic optimization was much more acceptable than single-objective thermodynamic or economic optimization. Also, thermoeconomic analysis regarding engineering criteria could yield more satisfactory overall results. In another research, Xing et al. [3] carried out a performance evaluation of a CRC equipped with an ejector subcooled system. They proposed a novel ejector-enhanced CRC for mechanical subcooling to improve a conventional single-stage CRC performance. The analysis results showed that the novel ejector subcooling CRC achieves coefficient of performance (COP) improvements of 7.0% and 9.5% by using R290 and R404A as refrigerants, respectively, in comparison to that of the conventional single-stage CRC.

There are many ways to performance improvement of the CRC. One of these techniques is to use the ejector as an expansion device. The use of ejectors is preferred because of the lack of moving mechanical parts and, as a result, achieving very low depreciation with very high efficiency simultaneously. Nowadays, ejectors are widely used in many industrial applications, such as Rankine cycles in power plants and compression refrigeration systems. So far, a wide range of research has been investigated on the ejector-enhanced compression refrigeration cycles [4–7]. In this technique, the researchers use an ejector as an expansion device between the condenser and evaporator to prevent energy losses in the expansion process. The result is an improvement in the exergy efficiency and COP due to the energy loss reduction and refrigeration capacity increasing in the thermal cycle. Since 1930, ejector refrigeration systems have been used for cooling and air conditioning. At the time, the refrigerant of these systems was water vapor, which made them bulkier and reduced the COP of the cycle. With advances in mechanical compressor design and chlorofluorocarbons discovery, the use of the ejector system was stopped. Nowadays, these systems are being reconsidered because they can use renewable energy sources such as geothermal and solar energy, and also low-temperature energy sources such as thermal engines and industrial cycles waste heat recovery. Solar energy is one of the most popular renewable and sustainable energy sources, complementing social and environmental sustainability, widely used in cooling applications and Organic Rankine Cycle (ORC) for cooling and power generation [63,64]. So far, many researchers have investigated the effect of using solar energy in heating and cooling systems. Rodriguez-Pastor et al. [65] used TRNSYS dynamic simulation linked to an Engineering Equation Solver (EES) thermodynamic model to evaluate the impact of using ORC systems for electricity production in buildings with solar water heating systems. Razmi et al. [66] proposed a novel hybrid design for green hydrogen production/utilization, including heliostat solar field, solid oxide electrolyzer cell, and solid oxide fuel cell. They conducted thermodynamic and economic analyses on these efficient high-temperature units and achieved an overall round-trip efficiency of 74.2%. In another study, Han et al. [67] proposed a novel solar-aided power generation system based on the unique characteristics of nonconcentrating and concentrating solar energy applied to lignite drying. The new system achieved significantly better performance than the conventional system by efficiently utilizing diffused solar irradiance during cloudy days.

The ejector refrigeration system has advantages in comparison to compression refrigeration cycles. One of the benefits is that ejector refrigeration systems operate using the wasted heat energy generated in most industrial processes by burning fossil fuels. Therefore, these refrigeration cycles can work with recyclable thermal energy sources. Since these cycles can be set up using renewable and sustainable energies, they are also important from the environmental perspective to reduce the emission of non-environmentally friendly greenhouse gases. An ejector is a simplified vacuum compressor with no mechanical parts such as valves, rotors, or pistons. The principle of the ejector operation is based on the continuous conversion of kinetic energy to compressive energy in the fluid during the ejector cross-section. In 1901, the ejector was invented by Charles Parsons, and then it was used in the first refrigeration cycle by Maurice LeBlanc in 1910 [8]. In the ejector, the secondary fluid is driven by the primary fluid kinetic energy. The mixed fluid pressure at the ejector outlet is between the pressure values of the primary and secondary flow. Sarkar [9] investigated the effect of adding ejectors to improve the performance of CRCs and heat pump cycles. By considering the different conditions and geometries for the ejector and using these circumstances for the cycle's simulation, he observed a performance improvement in the thermal cycles compared to the conventional ones. Yadav et al. [10] proposed a solar-driven refrigeration cycle by using an adjustable jet-ejector equipped with R1234yf as refrigerant. They optimized the proposed thermal storage system by considering the influence of different thermal storage capacities and thermal power consumption strategies in the refrigeration cycle. Sadeghi et al. [11], by using an ejector instead of a compressor, designed a refrigeration system powered by a low-temperature combustion engine heat source. They conducted energetic, exergetic, and exergoeconomic analyses for the proposed cycle. They performed the genetic multi-objective optimization algorithm by considering two objective functions to find the cycle optimum operating conditions. Yan et al. [12] evaluated the performance of the cascade ejector CRC. The condensers of both sub-cycles are air-cooled, and the refrigerant R134a is used as working fluid. They performed many experiments on the effect of the

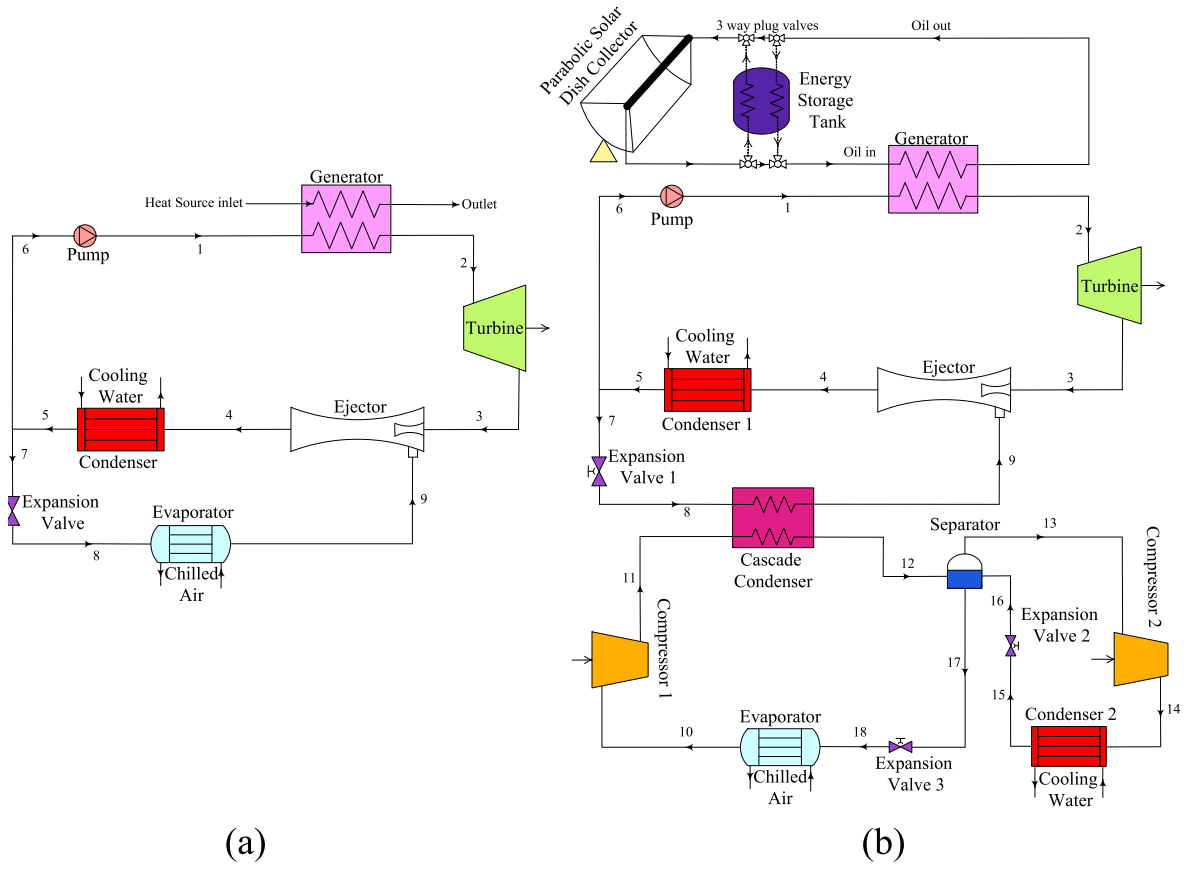

Fig. 1. Cycles schematic diagrams: (a) conventional Rankine power and ejector refrigeration cycle; (b) EORC-TCRC system.

evaporator, generator, and condenser temperatures on the performance of the cascade ejector CRC. The experiments results showed that the temperature of the evaporator, generator and condenser in each sub-cycle considerably affected the overall performance of the multi-stage system. The variation of the degree of sub-cooling at the cascade ejector CRC improves the COP more than the simple vapor CRC. Also, the result showed a 15.9 to 21 percent performance improvement in the COP at the optimum operating condition of the multi-stage refrigeration system. Yan et al. [13] investigated the energy and exergy analysis of a novel ejector-enhanced auto-cascade refrigeration system using R134a/R23 refrigerant mixture. They identified the compressor as the most prominent key component of the cycle exergy destruction. The exergy destruction of the compressor was evaluated at 25.1% and 23.11% in the simple and ejector-enhanced cycles, respectively. Also, using the ejector, the COP and efficiency of the second law improved by 8.42% and 18.02%, respectively. Sag et al. [14] experimentally evaluated the effect of using an ejector instead of an expansion valve on the CRC under ambient conditions and identical refrigeration capacity. The system's energetic and exergetic analysis was compiled using R134a as the operating fluid. They also identified the compressor as the thermal cycle's most crucial exergy destruction element. Using an ejector instead of an expansion valve resulted in 39–42% work recovery and improvement in the exergy efficiency and the COP with the ranges of 6.6–11.24% and 7.34–12.87%, respectively, which is a weakly result compared to Refs. [12,13]. The ejector scope of application is widely used as a vacuum device in many thermal cycles and industrial equipmentsequipment. One of the ejector applications is in the ejector-enhanced refrigeration systems. So far, much research has been investigated on the ejector refrigeration systems and the hybrid Rankine and ejector refrigeration systems. Chen et al. [15] investigated an experimental and theoretical analysis of an ejector refrigeration system. They presented the optimum temperature for the generator to achieve the highest Carnot efficiency in the cycle. They also found that the geometrical and thermodynamic properties of the ejector are susceptible, and changing these parameters can significantly affect the operating performance of the cycle. Lontsi et al. [16] proposed a novel cycle to produce multi-temperature cooling using combined ejector refrigeration and CRC. They found the proposed cycle could be a good alternative to the TCRC. Cao et al. [17] conducted thermo-economic analyses of a novel ejector booster-enhanced heat pump cycle. The results reveal that using R600/R143a as the system zeotropic mixture operating fluid can improve the COP of the proposed cycle up to 25% higher than the conventional cycle.

With a slight change in the ejector refrigeration cycle by adding a steam turbine before the ejector, a new system can be proposed based on cogeneration Rankine power and ejector refrigeration system [18–23]. In these studies, the scholars carried out affecting factors analysis in the cycle performance such as turbine inlet and outlet thermodynamic conditions, ejector entrainment ratio, and evaporator temperature. Using solar energy, Gupta et al. [24] integrated an EORC system with a triple pressure level absorption cycle. They established that with the addition of a triple pressure level absorption cycle in the ejector organic Rankine cycle, the energy efficiency of the whole system increases substantially while exergy efficiency decreases. In another research, Jannatkhah et al. [25] proposed a combined ORC and an ejector refrigeration system for the cogeneration heating, cooling, and power generation cycle in order to reduce the waste heat recovery of the diesel engine exhaust. They performed energetic and exergetic analyses of the proposed cycle, revealing the best exergetic efficiency for canola biodiesel by 53.95%.

This study presents a novel EORC-TCRC system based on a combined Rankine power and ejector refrigeration system integrated with a two-stage compression refrigeration system using solar energy. Nowadays, solar energy is highly regarded because of its nature as renewable and

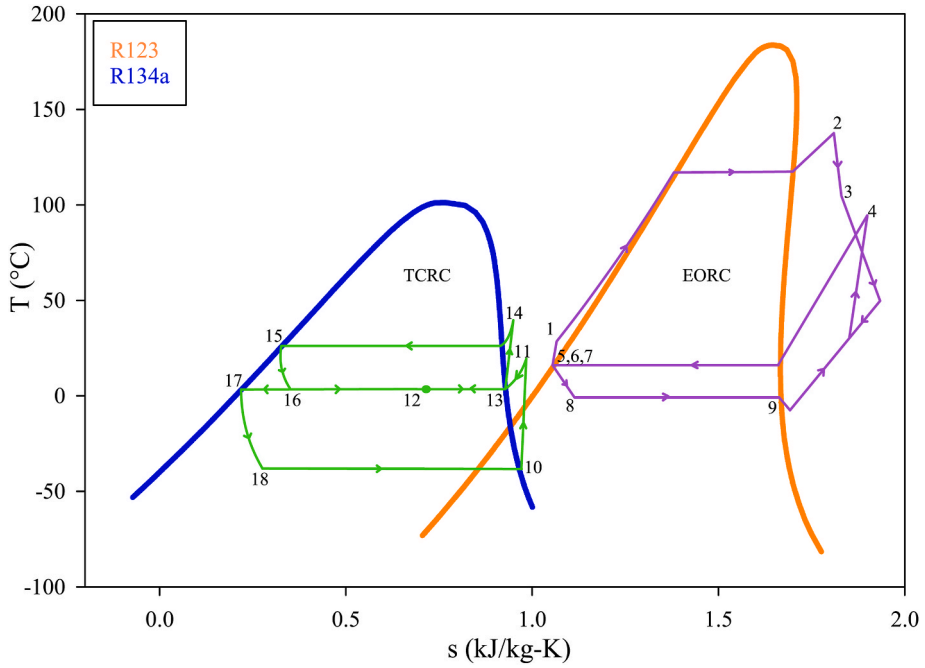

Fig. 2. T-s thermodynamic process diagram of the EORC-TCRC system.

sustainable energy. Even though solar collector usage and setting up solar systems have a higher initial cost, it removes fossil fuel consumption and the system's environmental costs; thus, system running and the thermal cycle maintenance costs are much less and more affordable. It is also momentous due to the lack of larger exergy-destructive components such as boiler stacks and higher thermal efficiency. Low-temperature cycles such as those used in organic operating fluids are among the best approaches to using clean, renewable, and sustainable energies. Hence, in this research, by implementing the cascade condenser technique, a novel cogeneration cycle is proposed based on an Ejector-enhanced Organic Rankine Cycle (EORC) integrated with a Two-stage Compression Refrigeration Cycle (TCRC).

Since ejector refrigeration cycles cannot produce refrigeration at very low temperatures, the main intention of offering this new system is to produce more refrigeration at lower evaporator temperatures using solar energy and thus achieve higher energetic and exergetic efficiency in the thermal cycle. The advantages of this novel EORC-TCRC system include higher thermal efficiency, higher exergy efficiency, and higher refrigeration production at lower chilled temperatures. Energy, exergy, economic, and environmental (4E) analyses of the novel EORC-TCRC system are investigated. Moreover, four modes of multi-objective optimizations using the NSGA-II method are conducted considering two decision variables (evaporator temperature and cascade condenser temperature) and three objective functions (energy efficiency, exergy efficiency, and the overall system cost rate) to achieve the optimal system performance in triple objective optimization scenarios. This new EORC-TCRC system utilizes an expansion ejector for the power cycle and the cascade condenser technology to achieve lower temperatures in the TCRC. The cascade system technology significantly solves significant thermal cycle efficiency limitations and challenges, such as efficient and safe expansion processes and higher isentropic efficiency dry turbine [61,62]. Thermodynamic and thermal-economic analysis of the cycle have been simulated by coding in the EES software, and the NSGA-II is implemented in MATLAB software coupling with EES by Dynamic Data Exchange (DDE) technique. This novel system uses ejector-enhanced ORC combined with TCRC via cascade condenser technique to propose a new efficient EORC-TCRC system. The results of the proposed system consist of a significant improvement in refrigeration output at lower evaporator temperatures, and gains the highest performance enhancement in both terms of energy and exergy efficiency in comparison to the other works.

2. System description

Fig. 1 depicts a schematic diagram of the conventional combined Rankine power and ejector refrigeration system and the novel EORC-TCRC system. First, the temperature of the operating fluid increases in the boiler by absorbing energy from the intermediate fluid, which is heated in the solar absorber collectors (state 1–2). Usually, water or industrial oils such as Therminol 66 are used as intermediate fluids in solar absorber collectors. Therminol 66 is one of the most popular oils in the world for heat transfer at high temperatures, and in the liquid phase, it is well stable at high temperatures. Hence, Therminol 66 is recommended for use in the solar energy base cycles due to its good stability even in the case of continuous working at the highest recommended temperatures in the system and also the capability of significant resistance to fouling and solid particle agglomeration and deposition in the system equipment. Furthermore, using this oil as an intermediate fluid in a parabolic trough collector makes it easy to generate superheated vapor in the vapor generator from the operating fluid in the ORC, even up to 300 °C. This superheated working fluid enters the turbine and consumes a part of its energy to produce power in the turbine (state 2–3).

The turbine outlet, which is still superheated flow, is the ejector's primary fluid. The ejector primary fluid converts its compressive energy into kinetic energy by passing through the initial convergent-divergent nozzle. Thus, the fluid velocity becomes supersonic. As a result of this process, a relatively low-pressure vacuum section is created. Hence, the secondary fluid is sucked into the mixing chamber. Therefore, this suction causes the evaporator's required pressure drop to evaporate the refrigerant. After the mixing process, the operating fluid's pressure increases by passing through the ejector diffuser. Fluid pressure at the ejector exit is between the primary and secondary flow pressure (state 3,9-4). In the following, the working fluid is condensed by passing through condenser 1 (state 4–5), and then a part of the flow is pumped to the vapor generator (state 6-1), and the other part by passing through expansion valve 1 directed to the evaporator to create refrigeration (state 8–9). In this novel cycle, the evaporator of the conventional

Table 1
Input parameters for the EORC-TCRC cycle modeling.

Parameters	Value	Unit
Hot oil's initial temperature	150	°C
Turbine inlet temperature	140	°C
Turbine inlet pressure	800	kPa
Turbine back pressure	200	kPa
Turbine isentropic efficiency	85	%
R123 mass flow rate ($\dot{m}_1$)	4.921	kg/s
R134a mass flow rate ($\dot{m}_{10}$)	1.5	kg/s
Ejector secondary flow temperature	−10	°C
Evaporator temperature	−30	°C
Pump isentropic efficiency	70	%
Primary nozzle isentropic efficiency (η_n)	90	%
Mixing chamber isentropic efficiency (η_m)	85	%
Diffuser section isentropic efficiency (η_d)	85	%

Table 2
Energy, exergy and exergy destruction equations for the EORC-TCRC system equipment.

Equipment	Energy balance	Exergy destruction
Boiler	$\dot{m}_{oil}\cdot(h_{oil,i}-h_{oil,o}) = \dot{m}_1\cdot(h_2-h_1)$	$\dot{I}_B = \dot{E}x_{oil,i} + \dot{E}x_1 - (\dot{E}x_{oil,o} + \dot{E}x_2)$
Turbine	$W_T = \eta_{T,s}\cdot\dot{m}_2\cdot(h_2-h_{3,s})$	$\dot{I}_T = \dot{E}x_2 - (\dot{E}x_3 + \dot{W}_T)$
Pump	$W_P = \dot{m}_6\dfrac{h_{1,s}-h_5}{\eta_{P,s}}$	$\dot{I}_P = \dot{E}x_6 - \dot{E}x_1 + \dot{W}_P$
Ejector	$\dot{m}_3h_3 + \dot{m}_9h_9 = \dot{m}_4h_4$	$\dot{I}_{Ej} = \dot{E}x_3 + \dot{E}x_9 - \dot{E}x_4$
Condenser 1	$\dot{Q}_{cond1} = \dot{m}_5\cdot(h_4-h_5)$	$\dot{I}_{cond1} = \dot{E}x_4 + \dot{E}x_{w,i,c1} - (\dot{E}x_5 + \dot{E}x_{w,o,c1})$
Condenser 2	$\dot{Q}_{cond2} = \dot{m}_{15}\cdot(h_{14}-h_{15})$	$\dot{I}_{cond2} = \dot{E}x_{14} + \dot{E}x_{w,i,c2} - (\dot{E}x_{15} + \dot{E}x_{w,o,c2})$
Cascade condenser	$\dot{m}_9\cdot(h_9-h_8) = \dot{m}_{11}\cdot(h_{11}-h_{12})$	$\dot{I}_{Cas.Cond} = \dot{E}x_8 + \dot{E}x_{11} - (\dot{E}x_9 + \dot{E}x_{12})$
Evaporator	$\dot{Q}_{evap} = \dot{m}_{18}\cdot(h_{10}-h_{18})$	$\dot{I}_{evap} = \dot{E}x_{19} - \dot{E}x_{10} + \dot{Q}_{evap}\left(1-\dfrac{T_0}{T_L}\right)$
Separator	$\dot{m}_{12}h_{12} + \dot{m}_{16}h_{16} = \dot{m}_{12}h_{17} + \dot{m}_{16}h_{13}$	$\dot{I}_{Se} = \dot{E}x_{12} + \dot{E}x_{16} - (\dot{E}x_{13} + \dot{E}x_{17})$
Expansion valve 1	$h_8 = h_7$	$\dot{I}_{expan1} = \dot{E}x_7 - \dot{E}x_8$
Expansion valve 2	$h_{16} = h_{15}$	$\dot{I}_{expan2} = \dot{E}x_{15} - \dot{E}x_{16}$
Expansion valve 3	$h_{18} = h_{17}$	$\dot{I}_{expan3} = \dot{E}x_{17} - \dot{E}x_{18}$
Compressor 1	$W_{C1} = \dot{m}_{10}\dfrac{h_{11,s}-h_{10}}{\eta_{C1,s}}$	$\dot{I}_{C1} = \dot{E}x_{10} + \dot{W}_{C1} - \dot{E}x_{11}$
Compressor 2	$W_{C2} = \dot{m}_{13}\dfrac{h_{14,s}-h_{13}}{\eta_{C2,s}}$	$\dot{I}_{C2} = \dot{E}x_{13} + \dot{W}_{C2} - \dot{E}x_{14}$

Rankine power and ejector refrigeration system is used as a cascade condenser for the TCRC. In the TCRC, the refrigerant passes through compressor 1 and then is directed to the cascade condenser, where it undergoes some initial condensation (state 11–12). The output of the cascade condenser, which contains a two-phase mixture of the operating fluid, enters the liquid-vapor separator. This separator works simultaneously as a flash chamber and vapor mixing intercooler (states 12–13 and 16–17). The saturated vapor part of the working fluid moves to compressor 2 for secondary compression. Then, in condenser 2, it undergoes secondary condensation (state 14–15) and returns to the separator after passing through the expansion valve 2. Also, for the cycle completion, the saturated part of the mixture is directed from the separator to the expansion valve 3. It then goes to the evaporator to generate the cooling effect (state 18-10). Using the two-stage compression method not only significantly reduces the compressor power consumption in the simple CRC but also increases the refrigeration capacity at the lower chilled temperatures due to the two-stage condensation and expansion of the refrigerant.

3. Materials and methodology

The temperature-entropy (T-s) thermodynamic process diagram of the EORC-TCRC system is depicted in Fig. 2. R123 refrigerant is used in the ejector-enhanced Rankine power cycle loop (EORC), and R134a refrigerant is used in the two-stage compression refrigeration system loop (TCRC).

3.1. Thermodynamic modeling assumptions

The following assumptions based on the literature references have been taken for the system modeling:

1) All thermodynamic processes are considered steady state and steady flow, and the effects of kinetic energy, system piping pressure drop, components heat losses, and potential energy are neglected.
2) The output of condensers 1 and 2 is saturated liquid, and the output of the evaporator is saturated vapor. The condenser's saturation temperature is 20 °C, and the ambient temperature and pressure conditions are 15 °C and 101.35 kPa, respectively [18].
3) Boiler, cascade condenser, condensers, and evaporator are tube and shell heat exchangers. The condenser's heat exchanger is water-cooled, and the evaporator heat exchanger is air-chilled.
4) The correction factor for all heat exchangers is considered 0.9.
5) The expansion process in the cycle expansion valves is considered isenthalpic.

In order to model the EORC-TCRC cycle, some input parameters are needed, which are listed in Table 1 [18].

3.2. Energy and exergy analysis

The governing equations for the cycle simulation comprise the mass, energy, and exergy balance equations; which can be expressed as follows [26]:

$$\sum \dot{m}_i = \sum \dot{m}_e \tag{1}$$

$$\sum \dot{m}_i h_i + \dot{Q} = \sum \dot{m}_e h_e + \dot{W} \tag{2}$$

$$\sum \dot{E}x_i + \sum\left(1-\frac{T_0}{T_s}\right)\dot{Q}_s = \sum \dot{E}x_e + \dot{W} + \dot{I} \tag{3}$$

In these equations h, $\dot{Q}$, $\dot{W}$, and $\dot{I}$ denote enthalpy, heat transfer rate, work rate, and exergy destruction rate, respectively. In the exergy balance equation $\left(1-\frac{T_0}{T_S}\right)\dot{Q}_S$ refers to the exergy rate of heat transfer. This term of the exergy balance equation is considered only in the equipment involving heat transfer to the environment. $\dot{E}x$ is the thermophysical exergy flow rate and is obtained by the following relation:

$$\dot{E}x = \dot{m}(h - h_0 - T_0(s - s_0)) \tag{4}$$

The empirical relationship of Brunin et al. [27] has been used to calculate the isentropic efficiency of the compressor expressed as equation (5). In this equation P_i refers to the compressor suction pressure, and P_o mentions the compressor discharge pressure.

$$\eta_{is} = 0.874 - 0.0135\frac{P_o}{P_i} \tag{5}$$

The exergy balance equation can be used to calculate the exergy destruction rate of the cycle equipment. The necessary equations to conduct the energy, exergy, and exergy destruction analysis of the cycle components are listed in Table 2.

The energetic and exergetic efficiency of the EORC-TCRC cycle define as follows:

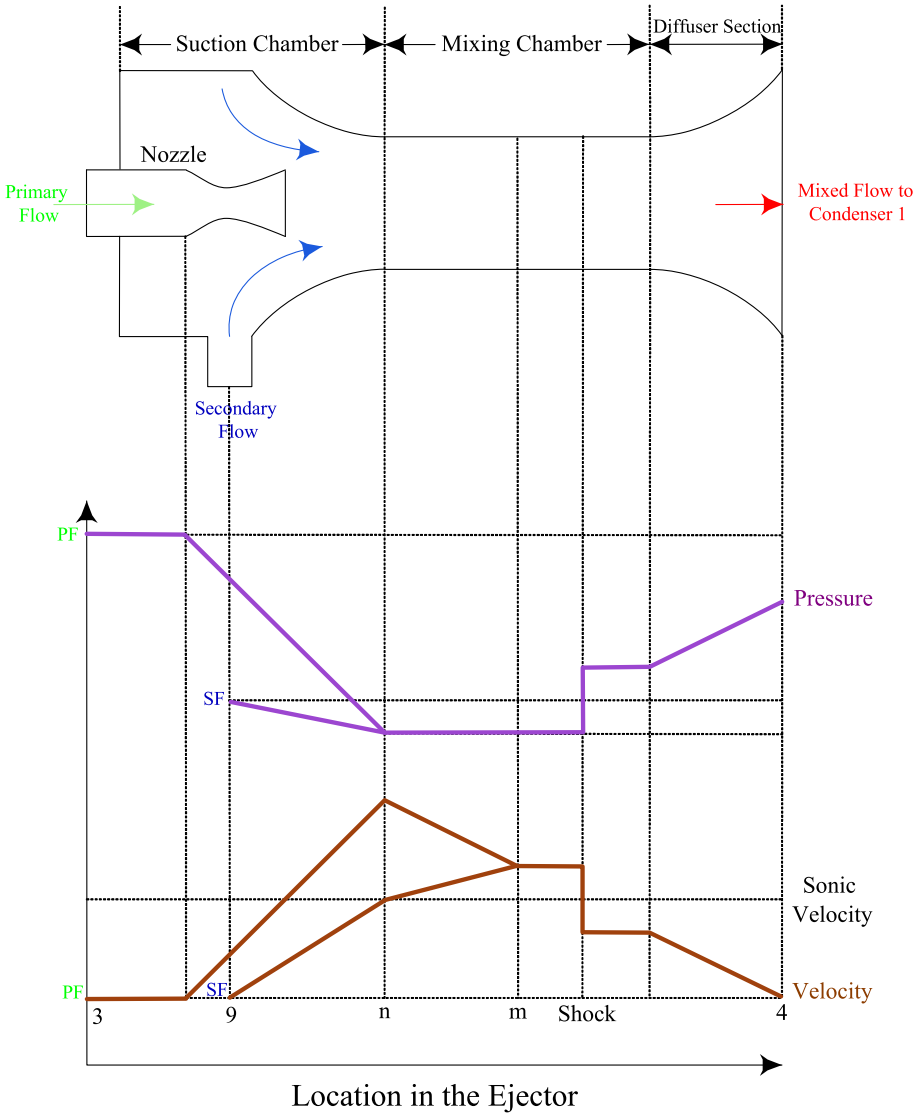

Fig. 3. Schematic diagram of the ejector geometric structural and different processes in the ejector.

$$\eta_{th} = \frac{\dot{W}_{net} + \dot{Q}_{evap}}{\dot{Q}_{in}} \tag{6}$$

$$\eta_{ex} = \frac{\dot{E}x_{out}}{\dot{E}x_{in}} = \left(1 - \frac{\dot{E}x_{des,total}}{\dot{E}x_{in}}\right) = \frac{\dot{W}_{net} + \dot{E}x_{evap}}{\dot{E}x_{in}} \tag{7}$$

Where $\dot{Q}_{in}$, $\dot{Q}_{evap}$, $\dot{W}_{net}$, $\dot{E}x_{evap}$, and $\dot{E}x_{in}$ represent the input thermal energy supplied to the system, the evaporator refrigeration capacity, the cycle net power output, the working fluid exergy difference in the evaporator, and the total input exergy to the cycle, respectively.

3.3. Ejector modeling development

So far, different models for ejector simulation have been proposed. Researchers use gas dynamics laws in some models to simulate and study the ejector performance by considering the ejector geometry. However, in many studies, researchers simulated the ejector by considering the isentropic efficiency of the primary nozzle, mixing chamber, and diffuser section to simplify the simulation process and reduce the computational time instead of engaging with the ejector geometry. Common models for ejector simulation are classified into the constant pressure of mixing and the constant cross-sectional area of mixing. The constant mixing pressure model is more prevalent in the scientific community due to its simplicity and more accurate prediction of the ejector performance. The basic principles of the constant mixing pressure model were proposed by Keenan et al. [28] based on gas dynamics and later generalized and developed by the research of Huang et al. [29] and Saleh [30]. In the current research, the constant pressure mixing model has been implemented for the ejector modeling. Flow is usually assumed to be one-dimensional for the ejector simulation in this method. A schematic diagram of the ejector geometric structure and the velocity and pressure distribution as a function of location along the ejector is illustrated in Fig. 3. By knowing the thermodynamic conditions of the ejector primary and secondary flow and applying the conservation of energy and momentum, the ejector outlet conditions can be determined. To simulate the ejector by constant pressure mixing model, the following assumptions have been considered [18]:

1) The ejector flow is steady state and one-dimensional.
2) The fluid velocity at the ejector inlet and outlet is ignored. Also, the secondary flow velocity in section n is assumed to be negligible compared to the primary flow velocity.
3) For simplicity, the effects of flow losses due to friction and mixing process in the ejector's nozzle, mixing chamber, and diffuser section are considered as isotropic efficiency of the nozzle, mixing chamber, and diffuser.

Table 3
Governing equations of the ejector modeling.

Parameter	Governing Equation
Entrainment ratio	$\mu = \frac{\dot{m}_9}{\dot{m}_3}$
primary nozzle isentropic efficiency	$\eta_n = \frac{h_3 - h_n}{h_3 - h_{n,is}}$
Primary flow outlet velocity	$u_n = \sqrt{2 \times (h_3 - h_n)}$
Mixing chamber momentum conservation	$\dot{m}_3 u_n = (\dot{m}_3 + \dot{m}_9) u_{m,is}$
Mixing chamber isentropic efficiency	$\eta_{lm} = \frac{u_m^2}{u_{m,is}^2}$
Mixing chamber energy balance equation	$\dot{m}_3\left(\frac{u_n^2}{2} + h_n\right) + \dot{m}_9 h_9 = (\dot{m}_3 + \dot{m}_9)\left(\frac{u_m^2}{2} + h_m\right)$
Diffuser section isentropic efficiency	$\eta_d = \frac{h_{4,is} - h_m}{h_4 - h_m}$
Mixed flow velocity	$u_m = \frac{\sqrt{\eta_m}.u_{3b}}{1+\mu}$
Mixed flow enthalpy	$h_m = \frac{h_3 + \mu.h_9}{1+\mu} - \frac{u_m^2}{2}$
Mixed flow outlet enthalpy to condenser 1	$h_4 = \frac{1}{2}u_m^2 + h_m$

Table 4
Governing equations of the thermoeconomic analysis modeling.

Description	Function
Heat exchangers heat transfer rate [31]	$\dot{Q} = F_C U A \Delta T_{LMTD}$
Logarithmic mean temperature difference [31]	$\Delta T_{LMTD} = \frac{(T_{h_i} - T_{c_o}) - (T_{h_o} - T_{c_i})}{Ln[(T_{h_i} - T_{c_o})/(T_{h_o} - T_{c_i})]}$
Overall heat transfer coefficient [32]	$U = \left(\frac{1}{h_o} + F_o + \left(\frac{D_o}{2k_w}\right)Ln\left(\frac{D_o}{D_i}\right) + \left(\frac{D_o}{D_i}\right)F_i + \left(\frac{D_o}{D_i}\right)\left(\frac{1}{h_i}\right)\right)^{-1}$
Overall cost function [33]	$C_{Total} = \sum C_i \dot{E}x_i + CRF\sum Z_j$
Capital recovery factor [68]	$CRF = \frac{i(1+i)^n}{(1+i)^n - 1}$
Compressors capital cost function [34,35]	$Z_{comp} = \frac{39.5\dot{m}}{(0.9 - \eta_{is})}\left(\frac{P_o}{P_i}\right)Ln\left(\frac{P_o}{P_i}\right)$
Heat exchangers capital cost function [36]	$Z_k = 516.621A_k + 268.45$
Pump capital cost function [37]	$Z_P = 3540\dot{W}_P^{0.71}$
Turbine capital cost function [37]	$Z_T = 6000\dot{W}_T^{0.7}$
Overall system cost rate	$C_{Total} = CRF\varphi\left(\begin{matrix}Z_{boiler} + Z_{turbine} + Z_{cond1} + Z_{Cas.Cond} + Z_{pump} \\ + Z_{comp1} + Z_{comp2} + Z_{evap} + Z_{cond2}\end{matrix}\right) + t_{op}C_i^{el}(\dot{W}_{comp1} + \dot{W}_{comp2} + \dot{W}_{pump})$

4) Whenever the flow after the mixing process is supersonic, it is assumed that a compression shock wave occurs upstream of the diffuser inlet.
5) The mixing process in the ejector mixing chamber is isobaric and obeys the energy and momentum conservation rules.
6) The processes in the ejector are adiabatic, and it is assumed that the ejector will not have any heat transfer with the environment.

The ejector entrainment ratio is one of the key parameters of the ejector design. The governing equations of the ejector modeling are listed in Table 3 [18].

To solve the ejector equations, two approaches can be proposed. The first case is when the value of the entrainment ratio is known, in which case the equations are explicitly solved. The second case is when the aim is to gain a specific pressure value at the ejector outlet. In this approach, by guessing the initial value for the entrainment ratio, the equations are solved by trial and error until the desired outlet pressure is satisfied.

3.4. Thermoeconomic analysis model

Logarithmic mean temperature difference (LMTD) technique has been used to model the current cycles' heat exchangers. The LMTD is an ideal and suitable method for heat exchangers where cold and hot fluid's inlet and outlet temperatures can be calculated and determined. In economic analysis, by simultaneously considering both thermodynamic and heat transfer parameters and using thermoeconomic equations, the cost functions of each component in the thermal cycle could be determined. The required equations for the thermoeconomic analysis model are listed in Table 4.

The heat exchangers heat transfer rate equation has been used to calculate the total surface area required in the heat exchangers of the cycles. Where $\dot{Q}$, F_C, U, A and ΔT_{LMTD} represent heat exchanger heat transfer rate, correction factor, overall heat transfer coefficient based on the external surface, required surface area for heat transfer, and LMTD, respectively. In the LMTD equation, T_{h_i} and T_{h_o} are the temperature of the hot fluid at the inlet and outlet of the heat exchanger, respectively, and T_{c_i} and T_{c_o} are the temperature of the cold fluid at the inlet and outlet of the heat exchanger, respectively. In overall heat transfer coefficient equation, F_i, F_o, D_i, D_o, h_i, h_o, and k_w are internal and external fouling factor of the heat exchanger, internal and external pipe's diameter, internal and external convection heat transfer coefficient of the fluid and thermal conductivity of the pipe's wall, respectively.

In overall cost function C_i is the input exergy unit cost of external sources, which in this case includes only the electricity consumption of the cycle by the pump and compressors and Z_j is rates of the initial, maintenance and overhaul costs of the system components. C_{Total} is the overall cost function of the thermal cycle. Initial costs include the cost of purchasing heat exchangers, compressors, expansion valves, refrigerants, instrument devices and connection pipes and tubes, and other structural costs of the system. In capital recovery factor n and i are the expected system llifetimeand the annual interest rate, respectively. In othe verall system cost rate $Z_{Cas.Cond}$, C_i^{el} and t_{op} represent cascade condenser investment cost, unit cost of electrical exergy and system annual operational hours, respectively. Costs related to the maintenance and overhaul of the system components are usually considered as a fraction of the costs associated with the initial investment. For this purpose, the maintenance cost factor φ in the overall cost function has been used. In this research, i = 0.15, n = 10, $t_{op} = 5000\ (hr)$, $C_i^{el} = 0.075$ ($/KWh) and φ = 1.06 are considered [11,38]. Expenses related to expansion valves, ejector, refrigerant, connection pipes and tubes, instrument devices, and other structural costs of the system can be considered as 0.84 percent of the overall initial investment cost [36].

Chemical engineering plant cost index (CEPCI) is used to update all the cost values evaluated from the original year to the reference year [53]:

$$Cost\ at\ reference\ year = Original\ cost \times \frac{CEPEI_{reference}}{CEPEI_{Original}} \tag{8}$$

3.5. Environmental impact and solar-assisted analysis

In recent years, due to increasing concerns about environmental affairs, especially global warming and climate change, greenhouse gas emissions in energy systems have become more critical and received considerable attention. Factors such as gas turbines, various engine's waste heat, boiler stacks, and different power systems, such as S–CO_2 and Brayton cycle, have the most remarkable non-environmentally friendly impact. One of the best solutions to reduce this non-environmentally friendly impact is using renewable energy sources in the thermal cycles. So far, many researchers developed solar-aided thermal cycles to upgrade more efficient energy systems [39,40].

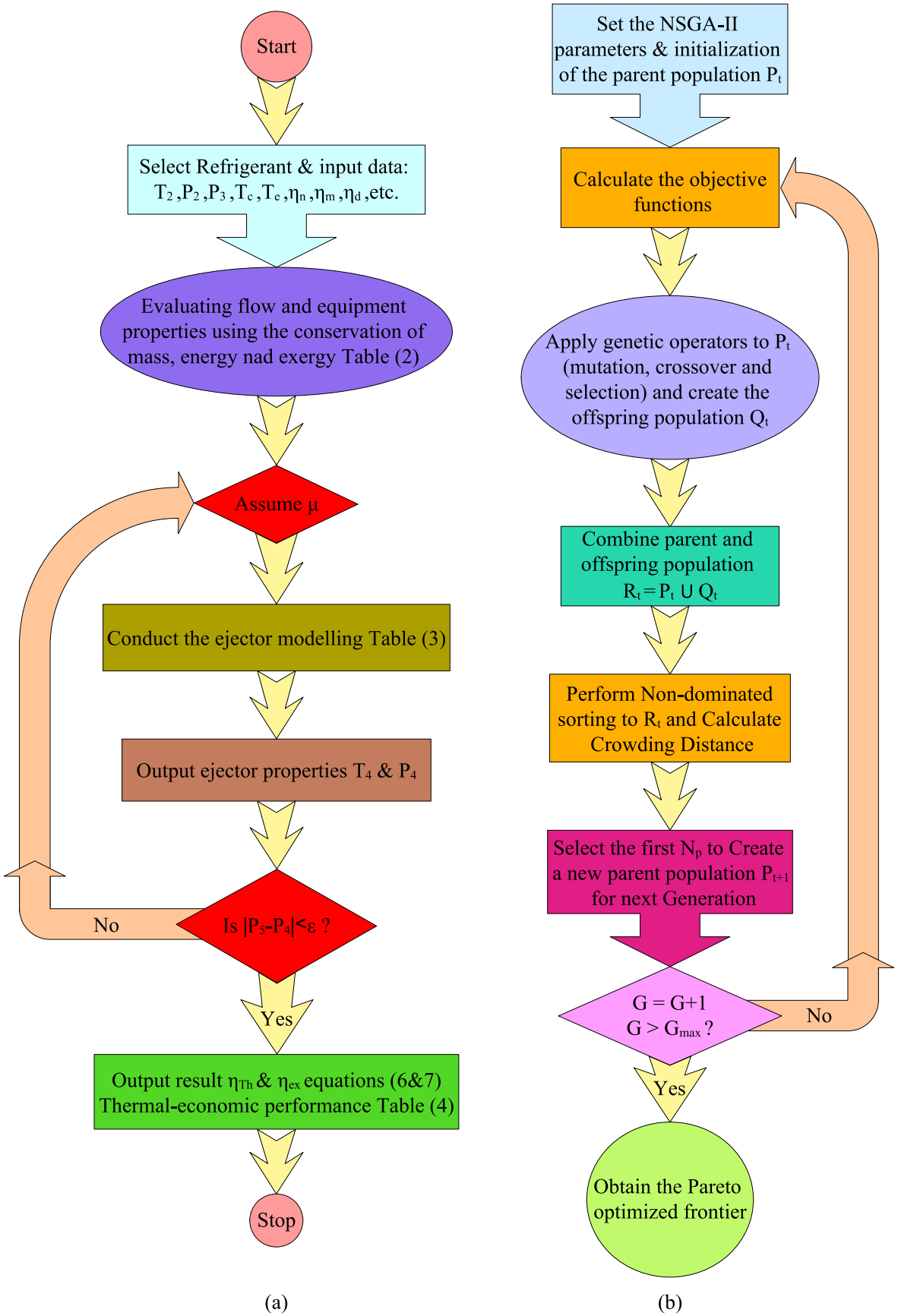

Fig. 4. The EORC-TCRC system simulation and optimization flowchart a) EES coding algorithm; b) NSGA-II multi-objective optimization algorithm.

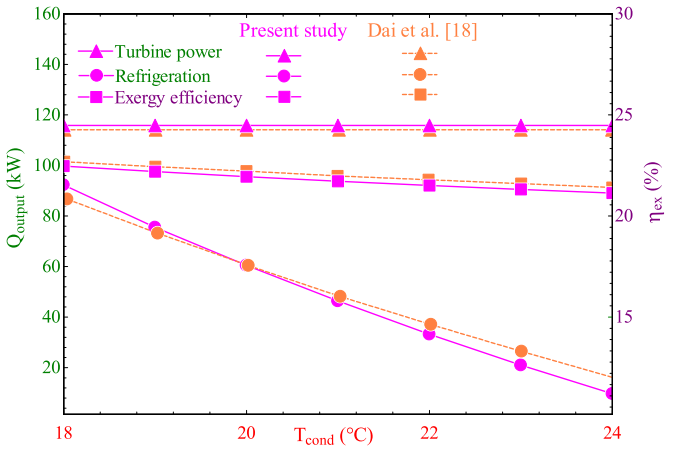

Fig. 5. Comparisons of turbine output power, exergy efficiency, and cooling capacity for various condenser temperatures.

Cogeneration Rankine cycle systems (RCSs) are the best approach for utilizing renewable energy sources. These thermal cycles increase the waste heat recovery potential and greenhouse gas emissions to the environment [41]. The CO_2 emission capital cost credit can be calculated as follows [42]:

$$Z_{CO_2} = z_{CO_2}.\varphi_{CO_2} \tag{9}$$

$$Z_{A_{CO_2}} = z_{CO_2}.\varphi_{A_{CO_2}} \tag{10}$$

Where Z_{CO_2}, $Z_{A_{CO_2}}$ and z_{CO_2} are the CO_2 capital cost credit per annum ($/yr), the specific

CO_2 capital cost credit ($/(yr.m^2)) and the CO_2 capital cost credit, respectively. The amount of CO_2 mitigated per annum φ_{CO_2} (kg/yr) and specific CO_2 mitigation per annum $\varphi_{A_{CO_2}}$ (kg/(yr.m^2)) can be expressed as follows [42]:

$$\varphi_{CO_2} = \psi_{CO_2}.E_t \tag{11}$$

$$\varphi_{A_{CO_2}} = \varphi_{CO_2} \Big/ A_{PV} \tag{12}$$

Where ψ_{CO_2}, E_t and A_{PV} are the average amount of CO_2 produced per kWh (kg/kWh) for fuel consumption, the net electrical gained by the cycle per annum (kWh/yr) and the surface area of the thermal system, respectively.

Cogeneration RCSs can provide an optimum solution from exergoeconomic and environmental points of view. These cycles also have improved in terms of output rates, exergy efficiency, and economic and environmental considerations. The major disadvantage of RCSs is their lower energy efficiency value [41]. One of the best approaches to enhancing the energy efficiency of RCSs is to use ORCs. ORC systems can work with any low-temperature energy source, especially renewable and sustainable energy sources such as solar energy.

The main idea of the current study is to present the novel EORC-TCRC system to achieve higher thermal and exergetic efficiency in the thermodynamic cycle. Also, due to the system's operation with solar energy, according to equations (9)–(12), the amount of greenhouse gas emissions in the cycle is zero, so the mentioned cycle is entirely environmentally friendly and has no destructive environmental impact. Hence, the significant interest of this study is to present and optimize a novel solar-assisted EORC-TCRC system, so this study does not go far into the details of calculating and designing the solar collector system. Due to the consideration of the inlet oil constant thermodynamic conditions as the cycle assumption, the constant value of solar heat capacity supplied to the generator and the initial investment costs of the solar system are considered as a constant value added to the generator cost.

3.6. Mathematical modeling development

The solving procedure of the EORC-TCRC system for conducting the 4E analysis and triple objective optimization is comprised of coding the mass, energy, and exergy balance equations for different components of the system (Table 2), assuming entrainment ratio and conducting the ejector modeling (Table 3) then calculating the system performance output (equation (6)&7), and finally performing the thermoeconomic model (Table 4) to obtain the 4E analysis of the thermal system. According to assumption No. 2 in the cycle description, the saturation temperature of condenser 1 is constant, so it is necessary that the pressure of the fluid at the ejector outlet must be equal to the saturation pressure at the condenser temperature; hence, the backflow does not occur in the ejector. Therefore, the ejector model uses an iteration loop to guess the initial value for the entrainment ratio and then applies trial and error until the desired outlet pressure is reached. All mathematical modeling and thermal-economic evaluation coding are conducted in the EES software. The flowchart for the EES coding algorithm to simulate the EORC-TCRC system is depicted in Fig. 4 (a).

3.7. Multi-objective optimization

In this investigation, the NSGA-II multi-objective optimization algorithm is carried out to achieve the optimum system performances on thermal efficiency, exergetic efficiency, and economic perspective. For the first time, the genetic optimization algorithm was developed by John Holland in the 1960s to simulate the growth and decay of living organisms [43]. Later, Deb et al. [44] used the elitism operator to propose the evolutionary optimization algorithm based on an elitist non-dominated sorting genetic algorithm known as NSGA-II. The elitist operator provides this opportunity for the elites of a population that can directly set as the next generation. This approach has made NSGA-II one of the popular optimization methods, especially in energy and industrial applications widely used by many researchers and scholars [45–57]. The flowchart of the NSGA-II algorithm is depicted in Fig. 4 (b). In an evolutionary loop of NSGA-II, first of all, the initial parent population is generated (P_t). Then, the offspring population Q_t is generated by applying genetic operators to P_t (mutation, crossover, and selection). Next, the parent and offspring populations are merged to create a larger population R_t, perform non-dominated sorting to R_t, and calculate crowding distance. Finally, by means of elitist sorting, individuals with better fitness are selected as the first N_p to create a new parent population P_{t+1} for the next generation. This NSGA-II loop is repeated until the maximum generation criteria are satisfied. A powerful MATLAB computational code is developed to conduct the NSGA-II optimization algorithm. By coupling the system output results from EES through the Dynamic Data Exchange (DDE) technique to MATLAB computational code, NSGA-II optimization is carried out, and the Pareto optimized frontier is obtained.

3.8. Model validation

To ensure the accuracy of the ejector model and the output results conducted by the EES simulation code, a subroutine is developed to model the conventional combined power and ejector refrigeration system Fig. 1 (a). Then, the results of turbine output power, exergy efficiency, and cooling capacity of this code are compared with the results of Dai et al. [18]. Fig. 5 compares turbine output power, exergy efficiency, and cooling capacity for various condenser temperatures. As can be seen, the EES simulation code output results are entirely consistent either qualitatively and quantitatively with Dai et al. results. The slight difference in the results can be due to errors in rounding numbers in the software calculations process and the minor difference in library sources and databases usage by different software to obtain the thermophysical properties of refrigerants. Thus, the provided EES simulation code to conduct the 4E analysis of the thermal EORC-TCRC system is perfectly

Table 5
Energetic and exergetic performance comparative analysis of the thermal cycles.

Result	Present study	Dai et al. [18]
Compressor 1 work (kW)	38.01	–
Compressor 2 work (kW)	34.1	–
Pump work (kW)	3.45	3.45
Turbine work (kW)	115.8	114.14
Net power output (kW)	40.24	110.69
Refrigeration output (kW)	280.5	60.44
Thermal efficiency (%)	25.39	13.72
Net power and refrigeration output (kW)	320.74	171.13
Exergy efficiency (%)	39.09	22.02

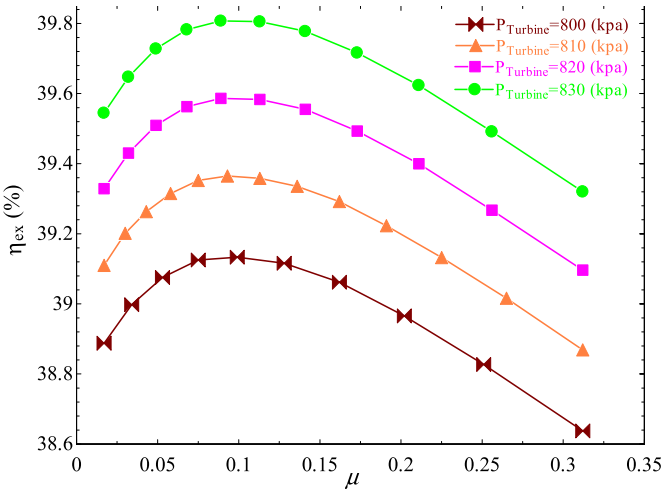

Fig. 6. Effect of entrainment ratio variations on the exergetic efficiency in different turbine pressures.

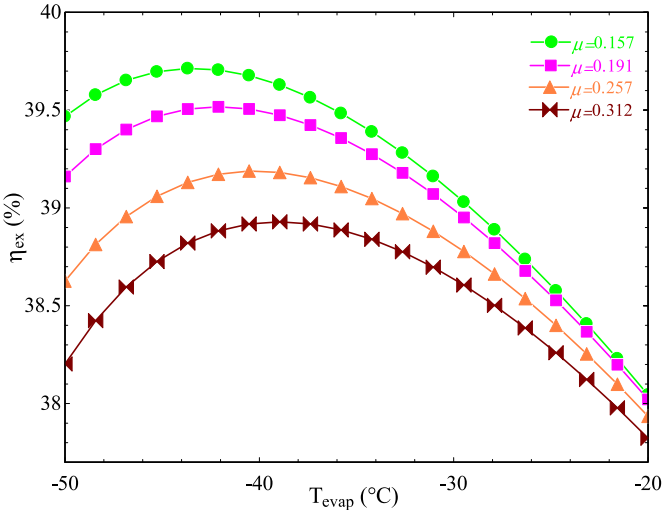

Fig. 7. Effect of evaporator temperature on the exergy efficiency in different ejector entrainment ratios.

validated and reliable.

4. Results and discussion

Table 5 demonstrates the results of the energetic and exergetic analysis of the EORC-TCRC system in comparison with the conventional combined Rankine power and ejector refrigeration system for the basic inputs parameters and thermodynamic conditions according to Table 1.

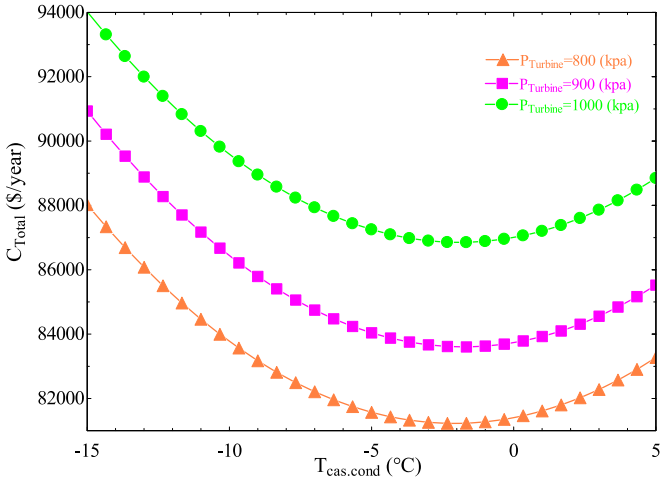

Fig. 8. Effect of cascade condenser temperature on the overall system cost rate in different turbine inlet pressures.

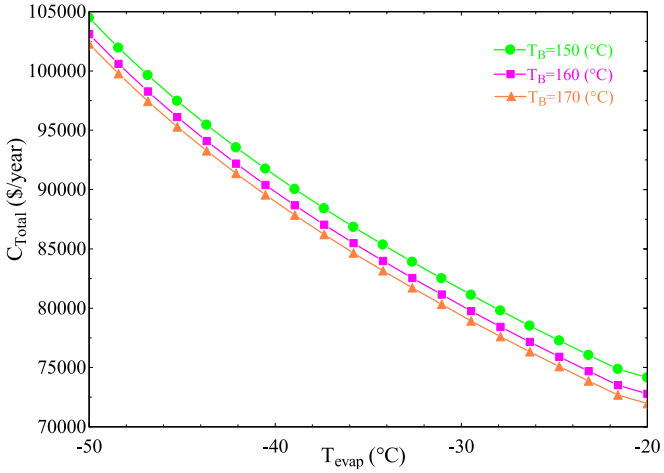

Fig. 9. Effect of evaporator temperature on the overall system cost rate in different generator inlet temperatures.

Table 6
The main considered parameters of the NSGA-II optimization procedure and the decision variables range.

Parameter	Values
Evaporator temperature	−50 to −15 °C
Cascade condenser temperature	−20 – 5 °C
Population size	200
Maximum number of generations	100
Mutation probability	0.2
Crossover probability	0.8

It is found that due to the lack of compressors in the conventional system, the net power output of the novel EORC-TCRC system is 63.65% less than the conventional cycle. At the same time, there is a significant increment in the energy efficiency, exergy efficiency, and cooling capacity of the EORC-TCRC cycle with values of 45.96%, 43.67%, and 78.45%, respectively.

A significant increment in the system cooling capacity and reduction in the total cycle exergy destruction will increase the thermal and exergetic efficiency, respectively.

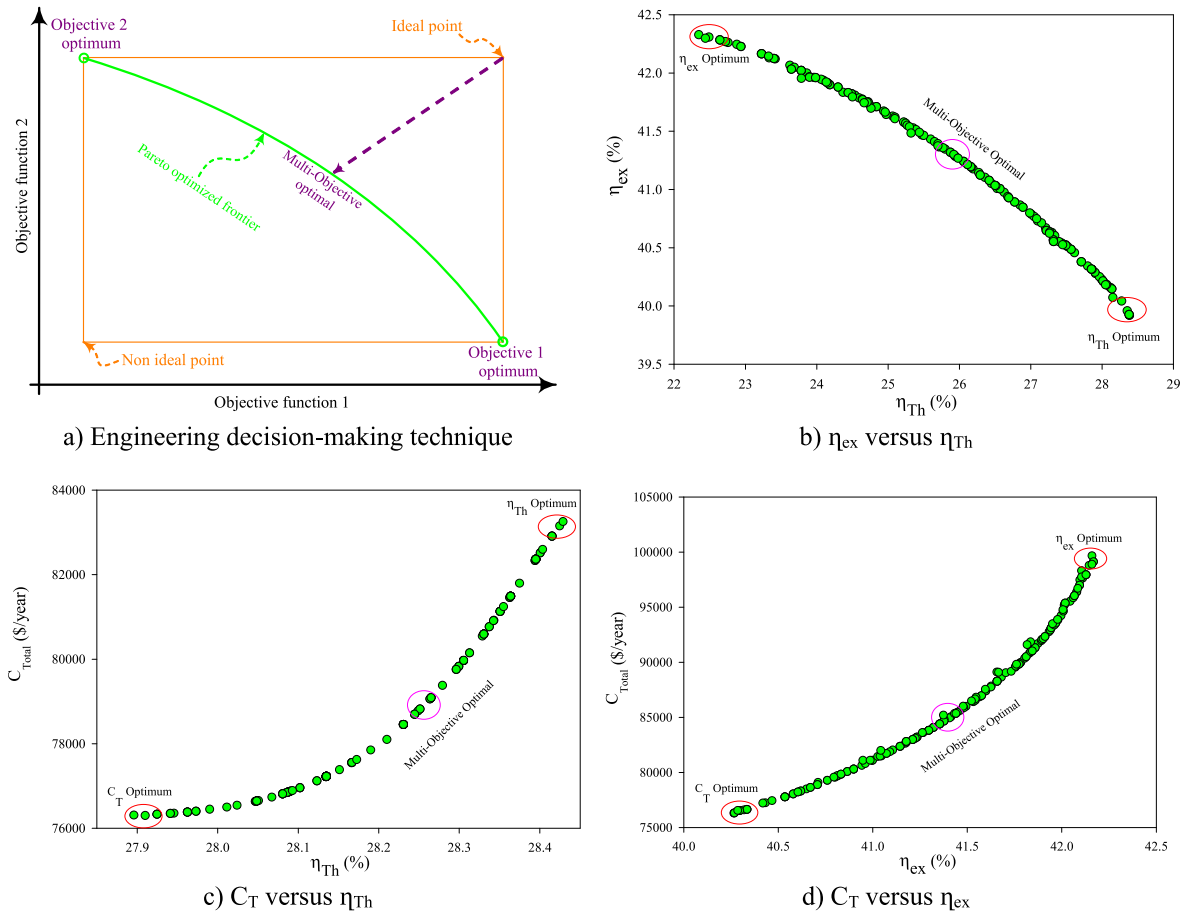

Fig. 10. Pareto optimized frontiers for Multi-Objective optimal system performance modes.

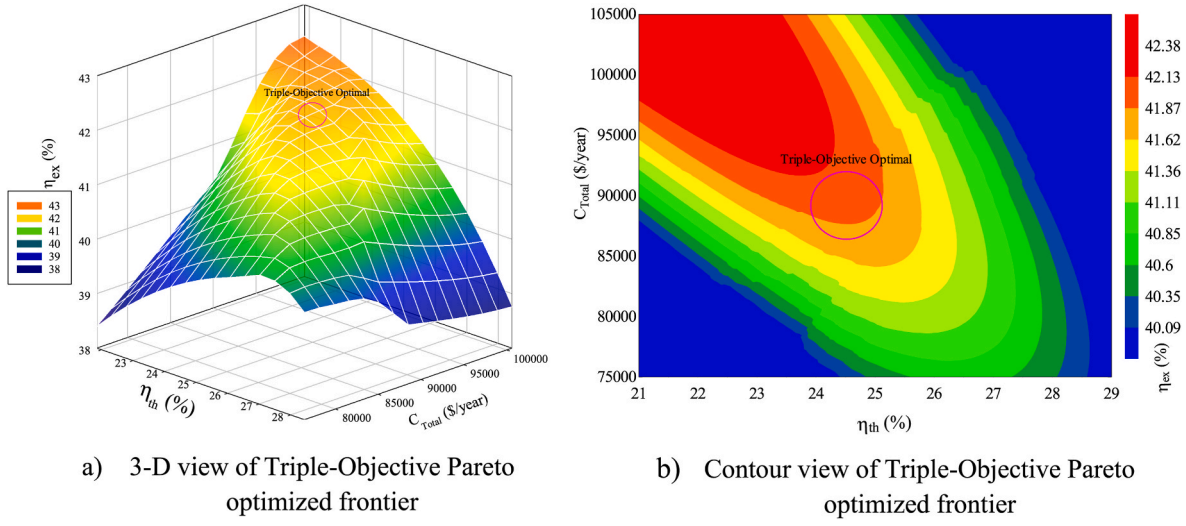

Fig. 11. Pareto optimized frontier for Triple-Objective optimal system performance mode.

4.1. Thermoeconomic results

Fig. 6 shows the effect of the entrainment ratio variations on the exergetic efficiency in different turbine inlet pressures. The ejector secondary flow temperature range is considered from −15 °C to 5 °C. As shown in Fig. 6, increasing the turbine inlet pressure increases the exergetic efficiency of the cycle. However, by increasing the entrainment ratio of the ejector, the exergetic efficiency first increases and then decreases. Therefore, there is a unique value for the entrainment ratio adapted to the maximum exergy efficiency.

Fig. 7 illustrates the impact of varying evaporator temperatures on exergetic efficiency across diverse ejector entrainment ratios. As evident in the figure, an incremental increase in the evaporator temperature leads to a rise in exergetic efficiency until it reaches a peak value, beyond which the efficiency starts to decline. This trend can be attributed to several underlying thermodynamic processes. Initially, the

Table 7
The optimum value of the system operating condition.

Design parameters	Multi-Objective η_{ex} - η_{Th}	Multi-Objective C_T - η_{Th}	Multi-Objective C_T - η_{ex}	Triple-Objective **η_{ex} - η_{Th} - C_T**
Evaporator temperature (°C)	−35.8	−20	−37.97	−35.86
Cascade condenser temperature (°C)	−12.65	−7.85	−6.36	−4.98
Thermal efficiency (%)	25.88	28.25	23.95	24.35
Exergy efficiency (%)	41.32	40.15	41.41	41.69
Overall system cost rate ($/year)	93,664	78,820	85,048	88,842

elevation in evaporator temperature results in a reduction of exergetic destruction by the low-pressure compressor. This phenomenon predominantly influences the exergetic efficiency at lower evaporator temperatures. However, as the evaporator temperature continues to ascend, there is a corresponding increase in the exergy destruction rate of the cycle compressors, particularly evident during higher temperature refrigeration production. This subsequently leads to a decrease in the overall exergetic efficiency of the cycle.

Another important point is that by increasing the entrainment ratio of the ejector, the maximum amount of exergy efficiency of the EORC-TCRC system occurs at the higher evaporator temperature. Fig. 8 shows the effect of cascade condenser temperature on the overall system cost rate in different turbine inlet pressures. With increasing turbine inlet pressure, the power production capacity and initial investment cost of the turbine increase. Also, more energy is needed to supply higher-pressure superheated vapor at the turbine inlet; therefore, the vapor generator heat capacity and the initial investment cost of the boiler also increase. As the cascade condenser temperature increases, the ejector entrainment ratio increases as well, which causes a reduction of the evaporator capacity and the high-pressure compressor power consumption. Therefore, the evaporator and high-pressure compressor costs are reduced.

On the other hand, by increasing the cascade condenser temperature, the low-pressure compressor power consumption and the cascade condenser capacity increase, which results in the overall system cost rate increment. This is why the overall system cost rate decreases first and then increases with the rise of the cascade condenser temperature, as shown in Fig. 8. Therefore, there is a specific value corresponding to the cascade condenser temperature and subsequently for the ejector entrainment ratio that the overall system cost rate reaches to its lowest value. This value is equivalent to the cycle optimal performance point from the economic perspective.

Fig. 9 illustrates the influence of the evaporator temperature on the overall system cost rate across varying generator inlet temperatures. As the vapor generator inlet temperature increases, there is a consequent rise in the LMTD within the boiler heat exchanger. This increase in LMTD leads to a reduction in the generator's capital cost rate and, subsequently, a decrease in the overall system cost rate.

Conversely, elevating the evaporator temperature results in a diminished capacity for Condenser 2 and a decrease in the compressor's power consumption. This reduction in capacity and power consumption subsequently leads to lower costs associated with these pieces of equipment, contributing further to the overall system cost rate reduction.

4.2. Multi-objective optimization results

In order to apply multi-objective optimization, the three most important parameters in the proposed system are chosen as objective functions. These three critical parameters are thermal efficiency, exergetic efficiency, and the overall system cost rate.

According to Figs. 6–8, it is found that the behavior of the overall system cost rate at the cascade condenser different temperatures is nonlinear convex. It can be seen that the behavior of the exergy efficiency at different temperatures of the evaporator and the cascade condenser is also nonlinear concave. Therefore, these two temperatures are selected as decision variables for multi-objective optimization for the proposed system. The NSGA-II considered operating parameters and the abovementioned decision variables range are listed in Table 6.

By considering different selections of the two objective functions, the Pareto-optimized frontiers obtained by NSGA-II are illustrated in Fig. 10. As can be seen, each objective function has an opposite variation trend compared to the other one. In evolutionary NSGA-II optimization results, each point of the Pareto-optimized frontier could be considered an optimal system operating condition, and none of the Pareto-optimized frontier points dominate the other. Hence, considering an engineering decision-making method, η_{Th} Optimum, η_{ex} Optimum, C_T Optimum, and multi-objective Optimal are chosen as the best energetic, exergetic, economic, and multi-objective system performance modes, respectively. In the engineering decision-making technique, the point closest to the ideal point on the Pareto optimized frontier could be considered the multi-objective optimal solution, as depicted in Fig. 10 (a).

Considering all three objective functions (η_{Th}, η_{ex}, and C_T), NSGA-II triple objective optimization of the presented EORC-TCRC system could be conducted. Fig. 11 demonstrated 3-D Pareto-optimized frontiers for triple objective optimization results. As can be seen, a specific area is selected as the triple objective optimized zone, which is closest to each one of the objective functions (maximum values of η_{Th} and η_{ex}, and minimum value of C_T). The final optimal system operating condition selected by engineering decision-making technique for each multi-objective and triple-objective optimization result is given in Table 7. It is found that the best system operating condition from thermal efficiency and overall system cost rate perspective occurs in multi-objective C_T - η_{Th} optimization mode with the values of 28.25 (%) and 78,820 ($/year), respectively. From the exergy efficiency perspective, the best system operating condition occurs in Triple-Objective η_{ex} - η_{Th} - C_T optimization mode with a 41.69 (%) value. It should be noted that the lowest and highest values of evaporator temperature occur in multi-objective C_T - η_{ex} and C_T - η_{Th} optimization modes with the values of −37.97 and −20 (°C), respectively.

Taking into account a better visual overview of the decision variables selection by NSGA-II in the last population of the feasible set, trend analysis of the scattered distribution of the decision variables is very important to setting more suitable engineering decision-making of the optimal system operating condition [58–60]. Hence, the scattered distribution of the decision variables compared to objective functions in the Pareto frontier is illustrated in Fig. 12.

It can be seen that most of the results have scattered distributions within the allowable decision variables range. However, for Multi-Objective C_T - η_{Th} mode, most of the optimization results have been obtained near the upper limit of the evaporator temperature Fig. 12 (b). Also, for the Triple-Objective mode, most of the optimal thermal efficiency, exergy efficiency, and overall system cost rate results are in the ranges of 24–25 %, 41.5–42 %, and 88,000–92,000 ($/year), respectively Fig. 12 (d), (e) and (f).

4.3. Selective triple -objective optimal point

The Sankey diagram of exergy flow distribution and thermodynamic properties of the state points for the selected Triple-Objective optimal system operating point are presented in Fig. 13 and Table 8, respectively. The generator, Ejector, and Condenser 1 are the three key components with the most extensive exergy destruction of the EORC-TCRC system, with values of 74.29 kW, 68.6 kW, and 54.04 kW, respectively, accounting for 17.65%, 16.29% and 12.84% of the overall system exergy input, respectively. In most energy systems, the generator has the

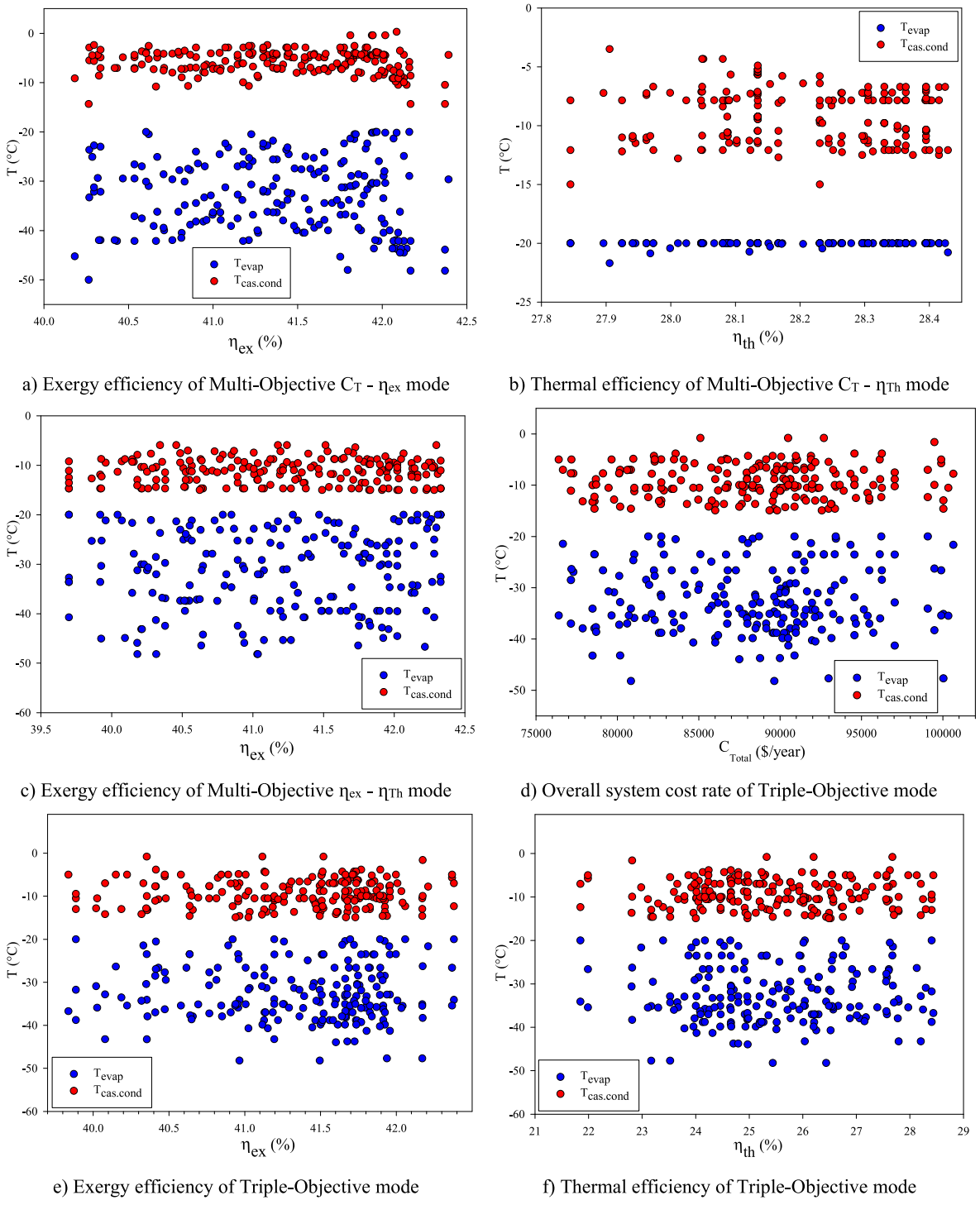

a) Exergy efficiency of Multi-Objective C_T - η_{ex} mode

b) Thermal efficiency of Multi-Objective C_T - η_{Th} mode

c) Exergy efficiency of Multi-Objective η_{ex} - η_{Th} mode

d) Overall system cost rate of Triple-Objective mode

e) Exergy efficiency of Triple-Objective mode

f) Thermal efficiency of Triple-Objective mode

Fig. 12. Scattered distribution of the decision variables in comparison with objective functions.

highest contribution to the total exergy destruction of the cycle due to the stack waste heat in the boiler exhaust and the high-temperature difference operating condition. Hence, it is essential to optimize the operating condition of such components, as well as reduce waste exergy by heat recovery processes and using clean energy sources such as geothermal and solar energy. The second component of the cycle with the highest value of exergy destruction is the ejector due to several irreversible processes, such as mixing, shock waves, and kinetic energy losses.

4.4. Comparative analysis and future perspective

Table 9 demonstrates a comparative analysis to determine the position of the current research in comparison to the other works.

As can be seen, the proposed cycle in the current study achieved the highest performance enhancement in both terms of energy and exergy efficiency.

The presented EORC-TCRC system is an alternative to conventional combined power and ejector refrigeration systems. The apparent advantages of using the cascade condenser technique to combine ejector-enhanced ORC with TCRC are a significant improvement in

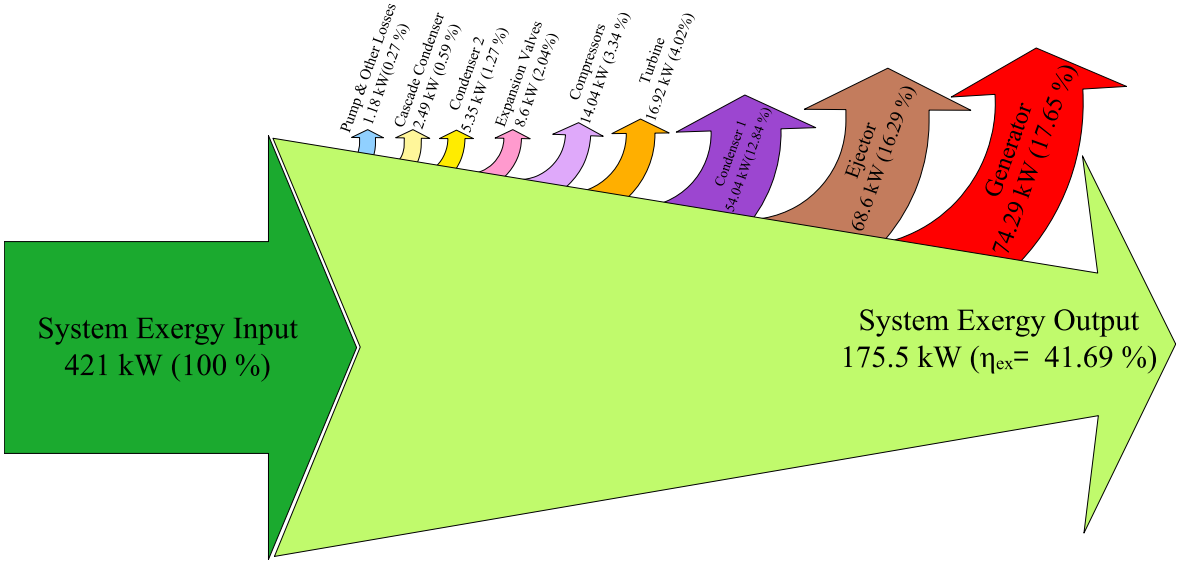

Fig. 13. Sankey diagram of exergy flow distribution for the Triple-Objective optimal system operating point.

Table 8
The thermodynamic parameters of the Triple-Objective optimal system operating condition.

State	Refrigerant	T (°C)	P (kPa)	$\dot{m}$ (kg/s)	h (kJ/kg)	s (kJ/kg.K)	$\dot{E}x$ (kW)
1	R123	20.51	900	4.921	221.8	1.075	2.984
2	R123	140	900	4.921	477.1	1.775	266.6
3	R123	99.15	200	4.921	451.9	1.787	125.7
4	R123	87.47	75.72	4.921	444.5	1.818	49.93
5	R123	20	75.72	4.921	221	1.074	0.232
6	R123	20	75.72	4.921	221	1.074	0.2084
7	R123	20	75.72	4.921	221	1.074	0.02355
8	R123	−4.98	25.92	4.921	221	1.079	−0.6955
9	R123	−4.98	25.92	4.921	379.6	1.67	−7.226
10	R134a	−35.86	63.39	1.5	228.5	0.963	−10.26
11	R134a	17.92	293.2	1.5	266.4	0.9879	35.85
12	R134a	0.02	293.2	1.5	207.6	0.7745	39.89
13	R134a	0.02	293.2	1.5	250.5	0.9314	33.09
14	R134a	25.18	572.1	1.5	266.7	0.9397	52.02
15	R134a	20	572.1	1.5	79.32	0.3006	47.58
16	R134a	0.02	293.2	1.5	79.32	0.3049	45.88
17	R134a	0.02	293.2	1.5	51.88	0.2045	52.68
18	R134a	−35.86	63.39	1.5	51.88	0.2188	46.5

refrigeration output at lower evaporator temperatures and gain the highest performance enhancement in both terms of energy and exergy efficiency in comparison to the other works.

Since R123 and R134a are recognizable as environmentally friendly, nonflammable, noncorrosive, and nontoxic working fluids, it is highly recommended that this novel system be used in practical application. Furthermore, for practical and industrial applications, it is recommended to conduct experimental analysis to investigate the effect of the unsteady state behavior of the dynamic system response.

5. Conclusions

This paper proposed a novel EORC-TCRC system based on a combined power and ejector refrigeration cycle integrated with a two-stage compression refrigeration cycle. 4E analysis and triple objective optimization were conducted to evaluate thermoeconomic performance and optimal system operating conditions. Energy and exergy analysis results under basic input parameters of Table 1 indicated significant improvement in refrigeration output, thermal efficiency, and exergy efficiency with values of 220.06 kW, 11.67%, and 17.07%, respectively, compared to the conventional power and ejector refrigeration cycle (Table 1, Die et al. [18]).

A list of the specific major findings reported here;

1. The presented cycle has been optimized using an evolutionary multi-objective NSGA-II optimization algorithm;
2. The results of the multi-objective C_T - η_{Th} optimization mode indicated that the best thermal efficiency and overall system cost rate operating conditions are 28.25 (%) and 78,820 ($/year), respectively;
3. The best thermal efficiency and overall system cost rate are corresponding to the evaporator and the cascade condenser temperatures of −20 (°C) and −7.85 (°C), respectively;
4. The results of the Triple-Objective η_{ex} - η_{Th} - C_T optimization mode indicated that the best exergy efficiency is 41.69 (%) and ocours in the evaporator and the cascade condenser temperatures of −35.86 (°C) and −4.98 (°C), respectively;
5. While the optimal system operating condition occurs in the Triple-Objective η_{ex} - η_{Th} - C_T mode from the exergy efficiency point of view, it costs 11.28% more and has 13.81% less energy efficiency compared to the multi-objective C_T - η_{Th} optimization mode;
6. However, in the Triple-Objective η_{ex} - η_{Th} - C_T mode, the evaporator temperature chills by 44.23% more than the multi-objective C_T - η_{Th} mode.

Table 9
The thermodynamic parameters of the Triple-Objective optimal system operating condition.

Research reference	Three key components of the most considerable exergy destruction			η_{Th} (%)	η_{ex} (%)
	Component I	Component II	Component III		
Current study	Generator (17.65%)	Ejector (16.29%)	Condenser 1 (12.84%)	24.35	41.69
Alirahmi et al. [60]	PTC (39%)	DWH (15%)	Chiller (14%)	18.69	31.99
Ebrahimi et al. [55]	CC (35.95%)	RG_1 (12.47%)	HEX_1 (10.36%)	–	31.41
Jamali et al. [43]	Comp II (19.20%)	Heater (13.96%)	Turbine (12.47%)	–	30.37
Wang et al. [21]	HRVG (56.51%)	Ejector (5.36%)	Turbine (5.07%)	14.92	27.51
Dai et al. [18]	Generator (51.89%)	Ejector (13.16%)	Condenser (9.45%)	13.72	22.2
Yang et al. [22,23]	Ejector (37.28%)	Generator (28.77%)	Condenser (17.18%)	10.77	9.76
Sadeghi et al. [11]	Generator (48.25%)	Ejector (38.11%)	Condenser (3.42%)	–	3.09

7. Accourding to the Sankey diagram of exergy flow distribution, the three key components with the most extensive exergy destruction are Generator, Ejector, and Condenser 1, with values of 74.29 kW, 68.6 kW, and 54.04 kW, respectively, accounting for 17.65%, 16.29% and 12.84% of the overall system exergy input, respectively;
8. According to the comparative analysis, the presented system has the best energy and exergy efficiency compared to the other works with a similar system as the current EORC-TCRC system.

It is strongly advised to conduct an experimental analysis on a pilot plant to utilize the Triple-Objective optimal system operating point for practical and industrial applications. Since the ejector is the second key component with the highest value of exergy destruction rate in the cycle, it is highly recommended for the future work to investigate the effect of using different working fluids, such as organic refrigerants and mixtures with two or more environmentally friendly substances to discover the best working fluids corresponding to the lowest value of the ejector irreversibility and exergy destruction rate.

CRediT authorship contribution statement

Hamed Mortazavi: Writing – original draft, Software, Conceptualization. **Hamidreza Mortazavy Beni:** Writing – review & editing, Investigation, Formal analysis. **Afshin Ahmadi Nadooshan:** Supervision, Resources. **Mohammad S. Islam:** Writing – review & editing, Visualization. **Mohammad Ghalambaz:** Writing – review & editing.

Declaration of competing interest

The authors of the manuscript hereby declare that they have no conflict of interest. The research was not funded by any organization or University.

Data availability

Data will be made available on request.

References

[1] Selbaş Reşat, Kızılkan Önder. Arzu Şencan, Thermoeconomic optimization of subcooled and superheated vapor compression refrigeration cycle. Energy 2006;31 (Issue 12):2108–28. https://doi.org/10.1016/j.energy.2005.10.015. ISSN 0360-5442.

[2] Sayyaadi Hoseyn, Nejatolahi Mostafa. Multi-objective optimization of a cooling tower assisted vapor compression refrigeration system. Int J Refrig 2011;34(Issue 1):243–56. https://doi.org/10.1016/j.ijrefrig.2010.07.026. ISSN 0140-7007.

[3] Xing Meibo, Yan Gang, Yu Jianlin. Performance evaluation of an ejector subcooled vapor-compression refrigeration cycle. Energy Convers Manag 2015;92:431–6. https://doi.org/10.1016/j.enconman.2014.12.091. ISSN 0196-8904.

[4] Li Huashan, Cao Fei, Bu Xianbiao, Wang Lingbao, Wang Xianlong. Performance characteristics of R1234yf ejector-expansion refrigeration cycle. Appl Energy 2014;121:96–103. https://doi.org/10.1016/j.apenergy.2014.01.079. ISSN 0306-2619.

[5] Wang F, Li DY, Zhou Y. Analysis for the ejector used as expansion valve in vapor compression refrigeration cycle. Appl Therm Eng 2016;96:576–82. https://doi.org/10.1016/j.applthermaleng.2015.11.095. ISSN 1359-4311.

[6] Lawrence Neal, Elbel Stefan. Theoretical and practical comparison of two-phase ejector refrigeration cycles including First and Second Law analysis. Int J Refrig 2013;36(Issue 4):1220–32. https://doi.org/10.1016/j.ijrefrig.2013.03.007. ISSN 0140-7007.

[7] Wang Xiao, Yu Jianlin, Zhou Mengliu, Lv Xiaolong. Comparative studies of ejector-expansion vapor compression refrigeration cycles for applications in domestic refrigerator-freezers. Energy 2014;70:635–42. https://doi.org/10.1016/j.energy.2014.04.076. ISSN 0360-5442.

[8] Ghorbani Bahram, Mafi Mostafa, Shirmohammadi Reza, Hamedi Mohammad-Hossein, Amidpour Majid. Optimization of operation parameters of refrigeration cycle using particle swarm and NLP techniques. J Nat Gas Sci Eng 2014;21:779–90. https://doi.org/10.1016/j.jngse.2014.10.007. ISSN 1875-5100.

[9] Sarkar Jahar. Ejector enhanced vapor compression refrigeration and heat pump systems—a review. Renew Sustain Energy Rev 2012;16(Issue 9):6647–59. https://doi.org/10.1016/j.rser.2012.08.007. ISSN 1364-0321.

[10] Manuel Luján José, Galindo José, Vicente Dolz, Ponce-Mora Alberto. Optimization of the thermal storage system in a solar-driven refrigeration system equipped with an adjustable jet-ejector. J Energy Storage 2022;45:103495. https://doi.org/10.1016/j.est.2021.103495. ISSN 2352-152X.

[11] Sadeghi Mohsen, Mahmoudi SMS, Saray R Khoshbakhti. Exergoeconomic analysis and multi-objective optimization of an ejector refrigeration cycle powered by an internal combustion (HCCI) engine. Energy Convers Manag 2015;96:403–17. https://doi.org/10.1016/j.enconman.2015.02.081. ISSN 0196-8904.

[12] Jia Yan, Cai Wenjian, Zhao Lei, Li Yanzhong, Lin Chen. Performance evaluation of a combined ejector-vapor compression cycle. Renew Energy 2013;55:331–7. https://doi.org/10.1016/j.renene.2012.12.029. ISSN 0960-1481.

[13] Yan Gang, Chen Jiaheng, Yu Jianlin. Energy and exergy analysis of a new ejector enhanced auto-cascade refrigeration cycle. Energy Convers Manag 2015;105:509–17. https://doi.org/10.1016/j.enconman.2015.07.087. ISSN 0196-8904.

[14] Bilir Sag N, Ersoy HK, Hepbasli A, Halkaci HS. Energetic and exergetic comparison of basic and ejector expander refrigeration systems operating under the same external conditions and cooling capacities. Energy Convers Manag 2015;90:184–94. https://doi.org/10.1016/j.enconman.2014.11.023. ISSN 0196-8904.

[15] Chen Jianyong, Havtun Hans, Palm Björn. Parametric analysis of ejector working characteristics in the refrigeration system. Appl Therm Eng 2014;69(Issues 1–2):130–42. https://doi.org/10.1016/j.applthermaleng.2014.04.047. ISSN 1359-4311.

[16] Lontsi F, Hamandjoda O, Sosso Mayi OT, Kemajou A. Development and performance analysis of a multi-temperature combined compression/ejection refrigeration cycle using environment friendly refrigerants. Int J Refrig 2016;69:42–50. https://doi.org/10.1016/j.ijrefrig.2016.05.018. ISSN 0140-7007.

[17] Cao Yan, Dhahad Hayder A, Mohamed Abdeliazim Mustafa, Anqi Ali E. Thermo-economic investigation and multi-objective optimization of a novel enhanced heat pump system with zeotropic mixture using NSGA-II. Appl Therm Eng 2021;194:116374. https://doi.org/10.1016/j.applthermaleng.2020.116374. ISSN 1359-4311.

[18] Dai Yiping, Wang Jiangfeng, Gao Lin. Exergy analysis, parametric analysis and optimization for a novel combined power and ejector refrigeration cycle. Appl Therm Eng 2009;29(Issue 10):1983–90. https://doi.org/10.1016/j.applthermaleng.2008.09.016. ISSN 1359-4311.

[19] Zheng B, Weng YW. A combined power and ejector refrigeration cycle for low temperature heat sources. Sol Energy 2010;84(Issue 5):784–91. https://doi.org/10.1016/j.solener.2010.02.001. ISSN 0038-092X.

[20] Hijriawan Miftah, Pambudi Nugroho Agung, Wijayanto Danar Susilo, Biddinika Muhammad Kunta, Huat Saw Lip. Experimental analysis of R134a working fluid on Organic Rankine Cycle (ORC) systems with scroll-expander. Engineering Science and Technology, an International Journal 2022;29:101036. https://doi.org/10.1016/j.jestch.2021.06.016. ISSN 2215-0986.

[21] Wang Jiangfeng, Dai Yiping, Sun Zhixin. A theoretical study on a novel combined power and ejector refrigeration cycle. Int J Refrig 2009;32(Issue 6):1186–94. https://doi.org/10.1016/j.ijrefrig.2009.01.021. ISSN 0140-7007.

[22] Yang Xingyang, Zhao Li, Li Hailong, Yu Zhixin. Theoretical analysis of a combined power and ejector refrigeration cycle using zeotropic mixture. Appl Energy 2015;160:912–9. https://doi.org/10.1016/j.apenergy.2015.05.001. ISSN 0306-2619.

[23] Yang Xingyang, Zheng Nan, Zhao Li, Deng Shuai, Li Hailong, Yu Zhixin. Analysis of a novel combined power and ejector-refrigeration cycle. Energy Convers Manag 2016;108:266–74. https://doi.org/10.1016/j.enconman.2015.11.019. ISSN 0196-8904.

[24] Gupta Devendra Kumar, Kumar Rajesh, Kumar Naveen. Performance analysis of PTC field based ejector organic Rankine cycle integrated with a triple pressure level vapor absorption system (EORTPAS), Engineering Science and Technology. Int J 2020;23(Issue 1):82–91. https://doi.org/10.1016/j.jestch.2019.04.008. ISSN 2215-0986.

[25] Jannatkhah Javad, Najafi Bahman, Ghaebi Hadi. Energy and exergy analysis of combined ORC – ERC system for biodiesel-fed diesel engine waste heat recovery. Energy Convers Manag 2020;209:112658. https://doi.org/10.1016/j.enconman.2020.112658. ISSN 0196-8904.
[26] Dincer Ibrahim, Rosen Marc A. Exergy, energy, environment and sustainable development, exergy. second ed. Elsevier; 2013 9780080970899 https://www.sciencedirect.com/book/9780080970899/exergy#book-description.
[27] Brunin O, Feidt M, Hivet B. Comparison of the working domains of some compression heat pumps and a compression-absorption heat pump. Int J Refrig 1997;20(Issue 5):308–18. https://doi.org/10.1016/S0140-7007(97)00025-X. ISSN 0140-7007.
[28] Keenan JH, Neumann EP, Lustwerk F.). "An investigation of ejector design by analysis and experiment. April 5 ASME. J. Appl. Mech. September 1950 2021;17 (3):299–309. https://doi.org/10.1115/1.4010131.
[29] Huang BJ, Chang JM, Wang CP, Petrenko VA. A 1-D analysis of ejector performance. Int J Refrig 1999;22(Issue 5):354–64. https://doi.org/10.1016/S0140-7007(99)00004-3. ISSN 0140-7007.
[30] Saleh B. Performance analysis and working fluid selection for ejector refrigeration cycle. Appl Therm Eng 2016;107:114–24. https://doi.org/10.1016/j.applthermaleng.2016.06.147. ISSN 1359-4311.
[31] Shah RK, Sekulic DP. Fundamentals of heat exchanger design. Canada: Wiley; August 2003. 978-0-471-32171-2.
[32] Florides GA, Kalogirou SA, Tassou SA, Wrobel LC. Design and construction of a LiBr–water absorption machine. Energy Convers Manag 2003;44(Issue 15): 2483–508. https://doi.org/10.1016/S0196-8904(03)00006-2. ISSN 0196-8904.
[33] Bejan A, Tsatsaronis G, Moran M. Thermal design and optimization. New York: Wiley; 1995. 978-0-471-58467-4.
[34] Valero Antonio, Lozano Miguel A, Serra Luis. George Tsatsaronis, Javier Pisa, Christos Frangopoulos, Michael R. von Spakovsky, CGAM problem: Definition and conventional solution. Energy 1994;19(Issue 3):279–86. https://doi.org/10.1016/0360-5442(94)90112-0. ISSN 0360-5442.
[35] Mosaffa AH, Garousi Farshi L. Exergoeconomic and environmental analyses of an air conditioning system using thermal energy storage. Appl Energy 2016;162: 515–26. https://doi.org/10.1016/j.apenergy.2015.10.122. ISSN 0306-2619.
[36] Jain Vaibhav, Sachdeva Gulshan, Singh Kachhwaha Surendra. Energy, exergy, economic and environmental (4E) analyses based comparative performance study and optimization of vapor compression-absorption integrated refrigeration system. Energy 2015;91:816–32. https://doi.org/10.1016/j.energy.2015.08.041. ISSN 0360-5442.
[37] Khaljani M, Khoshbakhti Saray R, Bahlouli K. Comprehensive analysis of energy, exergy and exergo-economic of cogeneration of heat and power in a combined gas turbine and organic Rankine cycle. Energy Convers Manag 2015;97:154–65. https://doi.org/10.1016/j.enconman.2015.02.067. ISSN 0196-8904.
[38] Jain Vaibhav, Sachdeva Gulshan, Singh Kachhwaha Surendra, Patel Bhavesh. Thermo-economic and environmental analyses based multi-objective optimization of vapor compression–absorption cascaded refrigeration system using NSGA-II technique. Energy Convers Manag 2016;113:230–42. https://doi.org/10.1016/j.enconman.2016.01.056. ISSN 0196-8904.
[39] Abdul Samad Farooq, Zhang Peng. Technical assessment, economic viability, and environmental impact of a solar-driven integrated space and water heating system in various configurations. Energy for Sustainable Development 2022;71:330–40. https://doi.org/10.1016/j.esd.2022.10.002. ISSN 0973-0826.
[40] Suresh MVJJ, Reddy KS. Ajit Kumar Kolar, 4-E (Energy, Exergy, Environment, and Economic) analysis of solar thermal aided coal-fired power plants. Energy for Sustainable Development 2010;14(Issue 4):267–79. https://doi.org/10.1016/j.esd.2010.09.002. ISSN 0973-0826.
[41] Tiktas Asli, Gunerhan Huseyin, Hepbasli Arif. Single and multigeneration Rankine cycles with aspects of thermodynamical modeling, energy and exergy analyses and optimization: a key review along with novel system description figures. Energy Convers Manag X 2022;14:100199. https://doi.org/10.1016/j.ecmx.2022.100199. ISSN 2590-1745.
[42] Fini Mehdi Alian, Gharapetian Derrick, Asgari Masoud. Efficiency improvement of hybrid PV-TEG system based on an energy, exergy, energy-economic and environmental analysis; experimental, mathematical and numerical approaches. Energy Convers Manag 2022;265:115767. https://doi.org/10.1016/j.enconman.2022.115767. ISSN 0196-8904.
[43] Jamali Arash, Ahmadi Pouria, Mohd Jaafar Mohammad Nazri. Optimization of a novel carbon dioxide cogeneration system using artificial neural network and multi-objective genetic algorithm. Appl Therm Eng 2014;64(Issues 1–2):293–306. https://doi.org/10.1016/j.applthermaleng.2013.11.071. ISSN 1359-4311.
[44] Deb K, Pratap A, Agarwal S, Meyarivan T. A fast and elitist multiobjective genetic algorithm: NSGA-II. IEEE Trans Evol Comput April 2002;6(2):182–97. https://doi.org/10.1109/4235.996017.
[45] Peng Li, Li Guoneng, Liu Jianyang, Su Hang, Han Xu, Han Zhonghe. Performance comparison and multi-objective optimization of improved and traditional compressed air energy storage systems integrated with solar collectors. J Energy Storage 2023;58:106149. https://doi.org/10.1016/j.est.2022.106149. ISSN 2352-152X.
[46] Habibi Hamed, Zoghi Mohammad, Chitsaz Ata, Javaherdeh Koroush, Ayazpour Mojtaba. Thermo-economic analysis and optimization of combined PERC - ORC - LNG power system for diesel engine waste heat recovery. Energy Convers Manag 2018;173:613–25. https://doi.org/10.1016/j.enconman.2018.08.005. ISSN 0196-8904.
[47] Golmohamadi Hessam, Keypour Reza, Mirzazade Pouya. Multi-objective co-optimization of power and heat in urban areas considering local air pollution, Engineering Science and Technology. Int J 2021;24(Issue 2):372–83. https://doi.org/10.1016/j.jestch.2020.08.004. ISSN 2215-0986.
[48] Saad Salim Mohammad, Kim Man-Hoe. Multi-objective thermo-economic optimization of a combined organic Rankine cycle and vapour compression refrigeration cycle. Energy Convers Manag 2019;199:112054. https://doi.org/10.1016/j.enconman.2019.112054. ISSN 0196-8904.
[49] Zhang Dongwei, Fang Chenglei, Shen Chao, Chen Songxuan, Li Hang, Xiang Qin, He Liu, Wu Xuehong. 4E analysis and multi-objective optimization of compression/ejection transcritical CO2 heat pump with latent thermal heat storage. J Energy Storage 2023;72(Part C):108475. https://doi.org/10.1016/j.est.2023.108475. ISSN 2352-152X.
[50] You Huailiang, Han Jitian, Liu Yang, Chen Changnian, Ge Yi. 4E analysis and multi-objective optimization of a micro poly-generation system based on SOFC/MGT/MED and organic steam ejector refrigerator. Energy 2020;206:118122. https://doi.org/10.1016/j.energy.2020.118122. ISSN 0360-5442.
[51] Mohammadi Hadelu Leila, Ahmadi Boyaghchi Fateme. Exergoeconomic and exergoenvironmental analyses and optimization of different ejector based two stage expander-organic flash cycles fuelled by solar energy. Energy Convers Manag 2020;216:112943. https://doi.org/10.1016/j.enconman.2020.112943. ISSN 0196-8904.
[52] Tahmasebzadehbaie Mohammad, Sayyaadi Hoseyn. Optimal design of a two-stage refrigeration cycle for natural gas pre-cooling in a gas refinery considering the best allocation of refrigerant. Energy Convers Manag 2020;210:112743. https://doi.org/10.1016/j.enconman.2020.112743. ISSN 0196-8904.
[53] Gantayet Amaresh, Kumar Dheer Dharmendra. A data-driven multi-objective optimization framework for optimal integration planning of solid-state transformer fed energy hub in a distribution network, Engineering Science and Technology. Int J 2022;36:101278. https://doi.org/10.1016/j.jestch.2022.101278. ISSN 2215-0986.
[54] Nateghi Seyedkeivan, Ali Mansoori, Amin Erfani Moghaddam Mohammad, Jan Kaczmarczyk. Multi-objective optimization of a multi-story hotel's energy demand and investing the money saved in energy supply with solar energy production. Energy for Sustainable Development 2023;72:33–41. https://doi.org/10.1016/j.esd.2022.11.010. ISSN 0973-0826.
[55] Ebrahimi-Moghadam Amir, Farzaneh-Gord Mahmood, Moghadam Ali Jabari, Nidal H, Abu-Hamdeh, Lasemi Mohammad Ali, Ahmad Arabkoohsar, Alimoradi Ashkan. Design and multi-criteria optimisation of a trigeneration district energy system based on gas turbine, Kalina, and ejector cycles: exergoeconomic and exergoenvironmental evaluation. Energy Convers Manag 2021;227:113581. https://doi.org/10.1016/j.enconman.2020.113581. ISSN 0196-8904.
[56] Yang Xuqing, Yang Shanju, Wang Haitao, Yu Zhenzhu, Liu Zhan, Zhang Weifeng. Parametric assessment, multi-objective optimization and advanced exergy analysis of a combined thermal-compressed air energy storage with an ejector-assisted Kalina cycle. Energy 2022;239(Part C):122148. https://doi.org/10.1016/j.energy.2021.122148. ISSN 0360-5442.
[57] Zuo Wei, Li Feng, Li Qingqing, Chen Zhijie, Huang Yuhan, Chu Huaqiang. Multi-objective optimization of micro planar combustor with tube outlet by RSM and NSGA-II for thermophotovoltaic applications. Energy 2024;291:130396. https://doi.org/10.1016/j.energy.2024.130396. ISSN 0360-5442.
[58] Shi Kelei, Asgari Armin. Energy, exergy, and exergoeconomic analyses and optimization of a novel thermal and compressed air energy storage integrated with a dual-pressure organic Rankine cycle and ejector refrigeration cycle. J Energy Storage 2022;47:103610. https://doi.org/10.1016/j.est.2021.103610. ISSN 2352-152X.
[59] Feng Yong-qiang, Zhang Wei, Hassan Niaz, Zhi-xia He, Wang Shuang, Wang Xin, Liu Yu-zhuang. Parametric analysis and thermo-economical optimization of a Supercritical-Subcritical organic Rankine cycle for waste heat utilization. Energy Convers Manag 2020;212:112773. https://doi.org/10.1016/j.enconman.2020.112773. ISSN 0196-8904.
[60] Alirahmi Seyed Mojtaba, Rahmani Dabbagh Sajjad, Ahmadi Pouria, Wongwises Somchai. Multi-objective design optimization of a multi-generation energy system based on geothermal and solar energy. Energy Convers Manag 2020; 205:112426. https://doi.org/10.1016/j.enconman.2019.112426. ISSN 0196-8904.
[61] Ren Xiao, Jing Li, Gao Guangtao, Pei Gang. An innovative concentrated solar power system driven by high-temperature cascade organic Rankine cycle. J Energy Storage 2022;52(Part B):104999. https://doi.org/10.1016/j.est.2022.104999. ISSN 2352-152X.
[62] Sanaye Sepehr, Khakpaay Navid. Thermo-economic multi-objective optimization of an innovative cascaded organic Rankine cycle heat recovery and power generation system integrated with gas engine and ice thermal energy storage. J Energy Storage 2020;32:101697. https://doi.org/10.1016/j.est.2020.101697. ISSN 2352-152X.
[63] Razmi Amir Reza, Alirahmi Seyed Mojtaba, Hossein Nabat Mohammad, Assareh Ehsanolah, Shahbakhti Mahdi. A green hydrogen energy storage concept based on parabolic trough collector and proton exchange membrane electrolyzer/fuel cell: thermodynamic and exergoeconomic analyses with multi-objective optimization. Int J Hydrogen Energy 2022;47(Issue 62):26468–89. https://doi.org/10.1016/j.ijhydene.2022.03.021. ISSN 0360-3199.
[64] Alshammari Saif, Kadam Sambhaji T, Yu Zhibin. Assessment of single rotor expander-compressor device in combined organic Rankine cycle (ORC) and vapor compression refrigeration cycle (VCR). Energy 2023;282:128763. https://doi.org/10.1016/j.energy.2023.128763. ISSN 0360-5442.
[65] Rodriguez-Pastor DA, Becerra JA, Chacartegui R. Adaptation of residential solar systems for domestic hot water (DHW) to hybrid organic Rankine Cycle (ORC) distributed generation. Energy 2023;263(Part D):125901. https://doi.org/10.1016/j.energy.2022.125901. ISSN 0360-5442.

[66] Razmi Amir Reza, Hanifi Amir Reza, Shahbakhti Mahdi. Design, thermodynamic, and economic analyses of a green hydrogen storage concept based on solid oxide electrolyzer/fuel cells and heliostat solar field. Renew Energy 2023;215:118996. https://doi.org/10.1016/j.renene.2023.118996. ISSN 0960-1481.

[67] Han Yu, Sun Yingying, Wu Junjie. An efficient and low-cost solar-aided lignite drying power generation system based on cascade utilisation of concentrating and non-concentrating solar energy. Energy 2024;289:129932. https://doi.org/10.1016/j.energy.2023.129932. ISSN 0360-5442.

[68] Karacayli Ibrahim, Altay Lutfiye, Hepbasli Arif. A parametric study on energy, exergy and exergoeconomic assessments of a modified auto-cascade refrigeration cycle supported by a dual evaporator refrigerator. Energy 2024;291:130255. https://doi.org/10.1016/j.energy.2024.130255. ISSN 0360-5442.